PNAS
www.pnas.org

Supplementary Information for

pH-Degradable, Bisphosphonate-loaded Nanogels Attenuate Liver Fibrosis by Repolarization of M2-type Macrophages

Leonard Kaps[†,‡], Anne Huppertsberg[§], Niklas Choteschovsky[†], Adrian Klefenz[†], Feyza Durak[||], Babara Schrörs[||], Mustafa Diken[||], Emma Eichler[†], Sebastian Rosigkeit[†], Sascha Schmitt[§], Christian Leps[#], Alicia Schulze[£], Friedrich Foerster[†,‡], Ernesto Bockamp[†], Bruno G. De Geest[¶], Kaloian Koynov[§], Hans-Joachim Räder[§], Stefan Tenzer[#], Federico Marini[£], Detlef Schuppan[†,Δ,*], Lutz Nuhn[§,*]

[†] Institute for Translational Immunology and Research Center for Immune Therapy, University Medical Center, Johannes Gutenberg-University Mainz, 55131 Mainz, Germany;

[‡] Department of Internal Medicine I, University Medical Center of the Johannes Gutenberg-University Mainz, 55131 Mainz, Germany;

[§] Max Planck Institute for Polymer Research, 55128 Mainz, Germany;

[#] Institute for Immunology, University Medical Center of the Johannes Gutenberg-University Mainz, 55131 Mainz, Germany;

[¶] Department of Pharmaceutics and Cancer Research Institute Ghent (CRIG), Ghent University, Ghent 9000, Belgium;

[||] TRON - Translational Oncology at University Medical Center of the Johannes Gutenberg-University Mainz gGmbH, 55131 Mainz, Germany;

[£]Institute of Medical Biostatistics, Epidemiology and Informatics (IMBEI), University Medical Center, Johannes Gutenberg-University Mainz, 55131 Mainz, Germany;

[Δ] Division of Gastroenterology, Beth Israel Deaconess Medical Center, Harvard Medical School, Boston, MA 02215, United States.

* Corresponding authors: Detlef Schuppan and Lutz Nuhn

Email: detlef.schuppan@unimedizin-mainz.de and lutz.nuhn@mpip-mainz.mpg.de

This PDF file includes:

Supplementary text (1. Materials; 2. Methods; 3. Syntheses; 4. Nanogel Characterization; 5. In vitro Studies; 6. In vivo Studies)
Figures S1 to S34, Table S1
SI References

1. Materials

Unless otherwise stated, all chemicals were obtained from commercial sources, such as Sigma Aldrich (Taufkirchen, Germany), TCI Chemicals (Tokyo, Japan) or Rapp Polymere (Tübingen, Germany) and used as received. Fluorescent dye Oregon Green 488 cadaverine was purchased from Thermo Fisher Scientific (Waltham, MA, USA), while near-infrared (NIR) dyes 800RS N-Hydroxysuccinimide (NHS) ester and 800RS cadaverine were obtained from Li-Cor Biosciences (Lincoln, NE, USA).
Solvents (HPLC grade) were purchased from Acros Organics (Geel, Belgium) and Fisher Scientific. Deuterium oxide was obtained from Sigma Aldrich. Millipore water was prepared using a MILLI-Q® Reference A+ System. For dialysis Spectra/Por7 dialysis membranes obtained from Spectrum Labs with a molecular weight cut off of 1000 g/mol were used.

2. Instrumentation

^{1}H, and ^{31}P NMR spectra were recorded at room temperature on a Bruker Avance III 300 MHz spectrometer. The chemical shifts (δ) are given in parts per million (ppm) relative to TMS. NMR spectra were processed with the software MestReNova 11.0.4 by Mestrelab Research. Samples were prepared in deuterated solvents and their corresponding signals referenced to residual non-deuterated solvent signals.
UV absorbance and fluorescence spectra were recorded using a Spark 20M Multimode Microplate Reader from Tecan Trading AG (Mannedorf, Switzerland).
Size-exclusion chromatography was performed using the following set-up: a PU2080+ pump, an auto sampler AS1555, an UV detector UV2075+ and a RI-detector RI2080+ from JASCO. Hexafluoroisopropanol (HFIP) containing 3.0 g/L of potassium trifluoroacetate was used as eluent at a flowrate of 0.8 mL/min and a column temperature of 40 °C. The column material was composed of modified silica obtained from MZ-Analysentechnik: PFG columns, particle size: 7 µm, porosity: 100 Å + 1000 Å. Relative molecular weight was determined by using a calibration with poly(methyl methacrylate) (PMMA) standards purchased from PSS (Mainz, Germany). Toluene was used as internal standard. Samples were prepared at 1 mg/mL and filtered through PVDF syringe filters (0.2 µm pore size, Acrodisc) prior to injection. The data was processed with the software PSS WINGPC UniChrom.
Electrospray Ionization Mass Spectrometry (ESI-MS) for NIR-labeled alendronate (NIR-AL) analysis was performed using a SYNAPT G2-Si Quadrupole-Ion Mobility-TOF MS (Waters Corporation, Milford, US). The instrument was calibrated by clusters of sodium formate in the mass range 50–2,000 m/z. Measurements were carried out at a capillary voltage of 3 kV, a sampling cone voltage of 80 V, a source offset of 80 V and a source temperature of 100 °C. Data processing was done by mMass (open-source mass spectrometry tool).
Prior to FCS measurements, fluorescently labeled nanogels were purified from residual unbound dye by spin-filtration. Therefore, Oregon Green-labeled alendronate-loaded nanogel (OG-AL/NP) dispersion (2 mg OG-AL/NP in 1 mL PBS) was purified using centrifugal filter units (regenerated cellulose, MWCO: 10,000 g/mol). After centrifugation PBS (0.8 mL) was added and centrifuged again. This procedure was repeated until complete disappearance of Oregon Green-derived absorbance in the filtrate was monitored by UV-Vis measurements.
To investigate the plasma stability 10 µL of nanogel dispersion (2 mg/mL OG-AL/NP in PBS) was incubated with 90 µL of human plasma at 37 °C under vigorous shaking. FCS data were recorded after 10 min and 24 h.
FCS measurements were performed using a commercial LSM880 setup (Carl Zeiss, Jena, Germany) equipped with a C-Apochromat 40x/1.2 W water immersion objective. An argon laser

(488 nm) was applied for excitation of Oregon Green. The fluorescence light was collected with the same objective and after passing a pinhole directed to a spectral detection unit (Quasar, Carl Zeiss). There, the light was spectrally separated by a grating element on a 32-channel array of GaAsP detectors operating in a single photon counting mode. Oregon Green emission was detected in the spectral range of 508-606 nm.
Measurements were performed in eight-well polystyrene-chambered coverglass (Laboratory-Tek, Nalge Nunc International, Penfield, NY, USA). The obtained FCS autocorrelation curves were fitted with the theoretical model function for an ensemble of one type of freely diffusing fluorescence species. The fits afforded the diffusion coefficients (*D*) of the studied species. Finally, the hydrodynamic radii (R_H) were calculated using the Stokes-Einstein relation: $R_H = \frac{k_B T}{6\pi\eta D}$, where k_B is the Boltzmann constant, T is the temperature, and η is the viscosity of the plasma.

3. Syntheses

3.1 Alendronate (AL) Synthesis

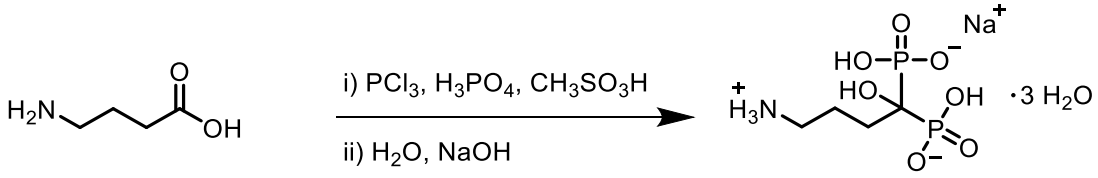

Fig. S1: Synthesis of alendronate (AL).

The synthesis of the bisphosphonate alendronate was conducted according to the protocol of G. R. Kieczykowski et al. (1).
In a three-neck round bottom flask equipped with a dropping funnel, reflux condenser and a stirring bar, 4-aminobutyric acid (10.0 g, 97.0 mmol, 1 eq.) and phosphorous acid (9.0 g, 97.6 mmol, 1 eq.) were dissolved in methanesulfonic acid (40 mL) under an inert nitrogen atmosphere. The mixture was warmed up to 65 °C, before phosphorus trichloride (18 mL, 205.8 mmol, 2.1 eq.) was added dropwise via dropping funnel over 20 min. Formed HCl was guided through $CaCl_2$. After the reaction mixture was maintained at 65 °C for 18 h, the clear colorless solution was cooled to RT and quenched into ice (100 g) with vigorous stirring. The reaction flask was rinsed with additional water (50 mL). The combined solution was refluxed for 6 h. After cooling and pH value adjustment to 2 using 50 % NaOH (80 mL) the reaction mixture was reduced to two thirds *in vacuo*. While the reduced reaction mixture was cooled on ice, a precipitate was formed, which was filtered off, washed with ice-cold water (20 mL) as well as 95 % ethanol (50 mL), and dried *in vacuo*. The product was obtained as monosodium trihydrate in the form of a white powder (24.3 g, 74.8 mmol, 77 %).
^{1}H-NMR (300 MHz, D_2O): δ (ppm) = 3.05 (t, *J* = 6.7 Hz, 2H, **a**), 2.19–1.80 (m, 4H, **b**).
^{31}P-NMR (121 MHz, D_2O): δ = 17.73.

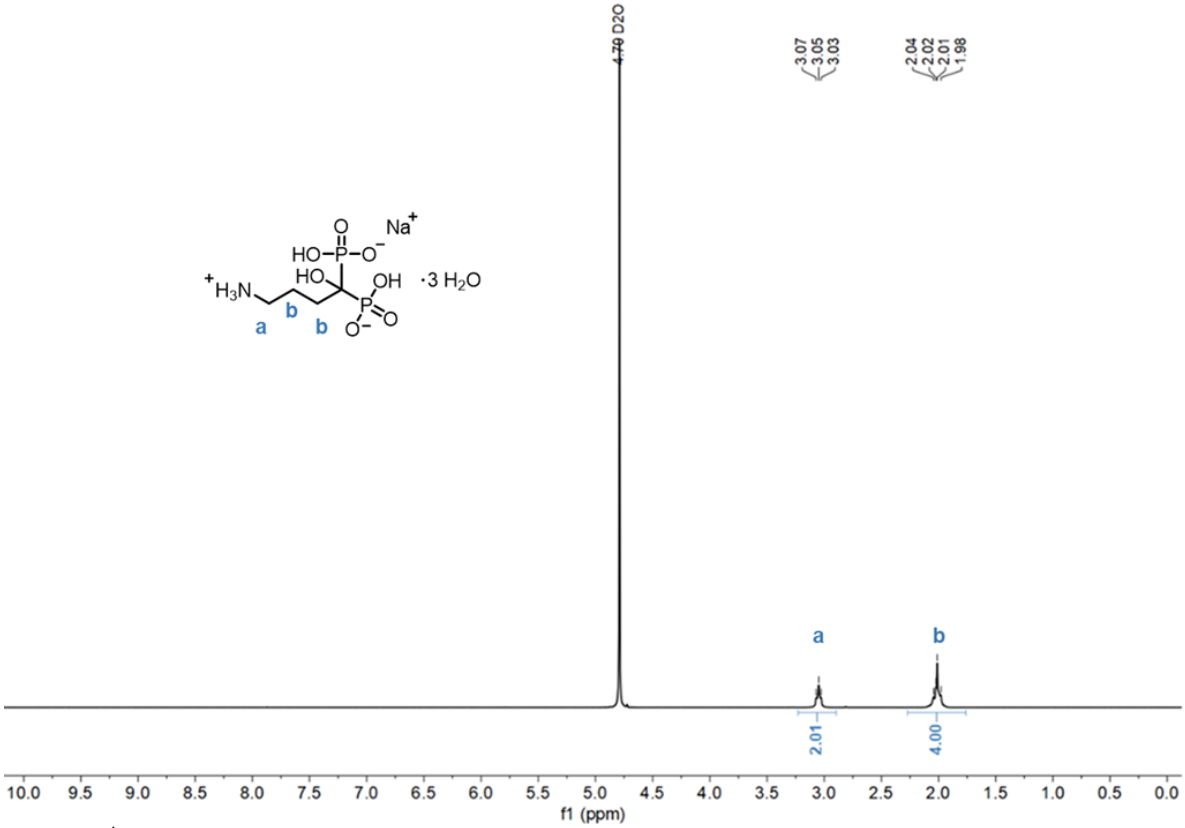

Fig. S2: ^{1}H-NMR spectrum (300 MHz) of alendronate (AL) in D_2O.

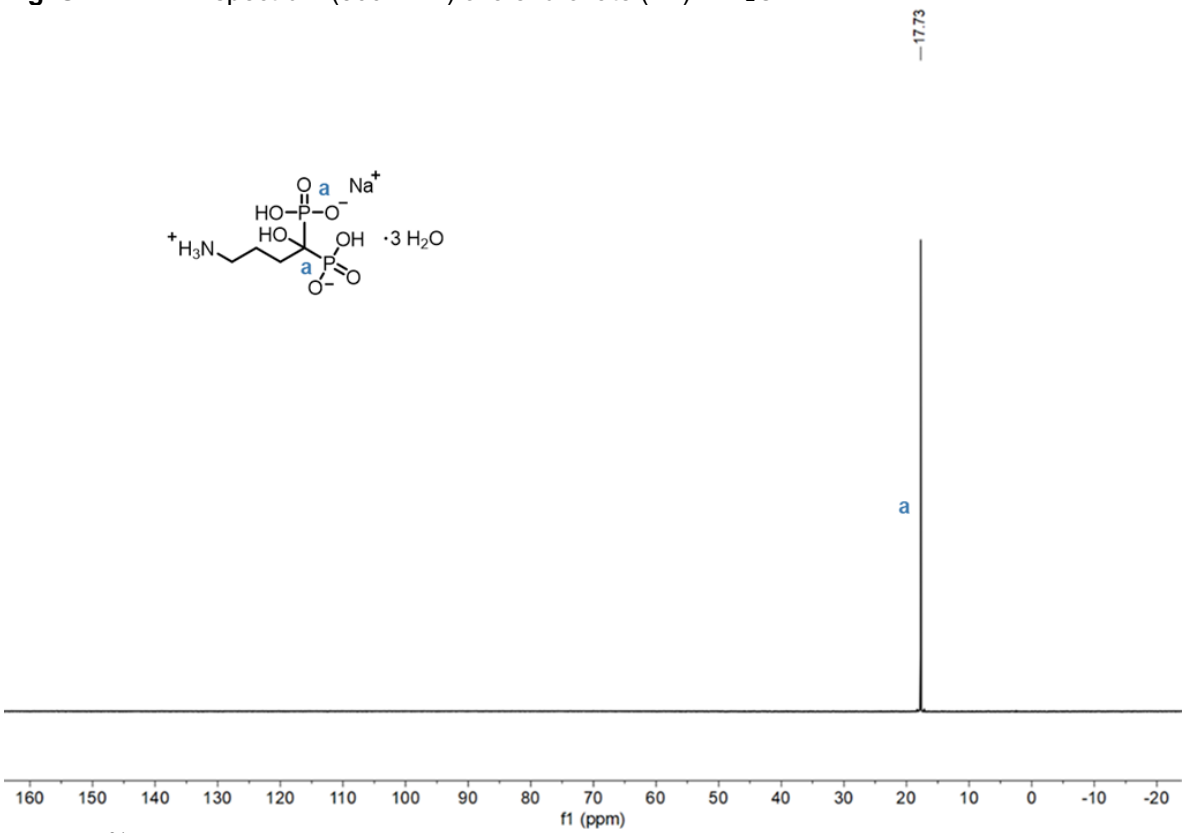

Fig. S3: ^{31}P-NMR spectrum (121 MHz) of alendronate (AL) in D_2O.

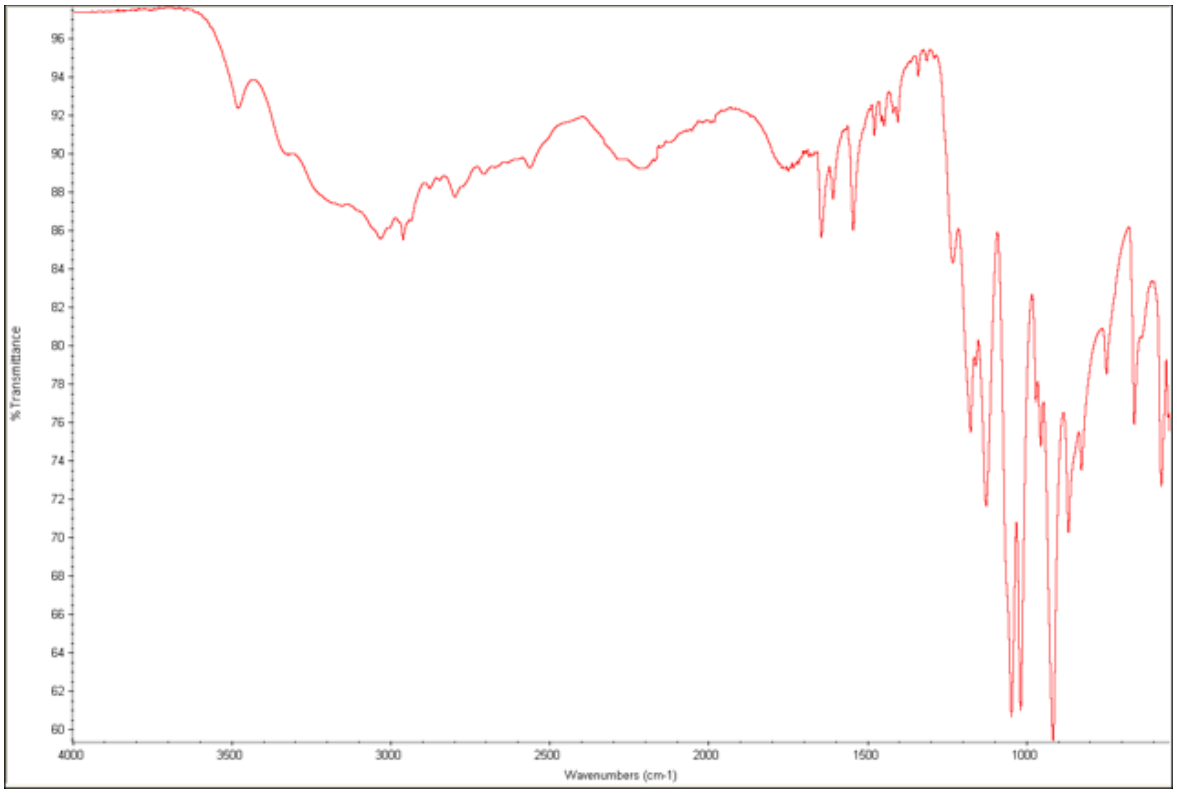

Fig. S4: IR spectrum of alendronate (AL).

3.2 Fluorescent Labeling of Alendronate (AL)

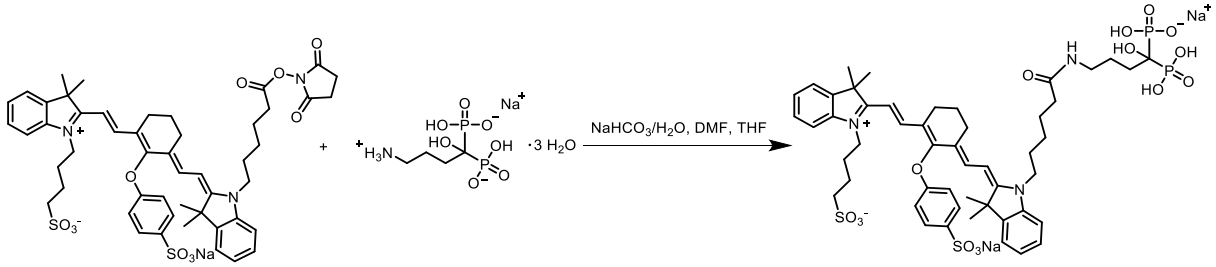

Fig. S5: Synthesis of NIR-labeled alendronate (NIR-AL).

In a 1.5 mL tube equipped with a stirring bar, alendronate (177.5 µg, 0.55 µmol, 1.05 eq.) was dissolved in 0.1 M $NaHCO_3$ (177.5 µL). After the NIR-dye 800RS-NHS ester (0.5 mg, 0.52 µmol, 1.0 eq.) was dissolved in DMF (25 µL) and THF (25 µL), the solution was added dropwise to the alendronate solution. After the reaction mixture was stirred at RT for 16 h under the protection of light, it was diluted with water (5 mL) and lyophilized. For further purification, the product was washed with ethanol (3 x 3 mL) and isolated by lyophilization. The conjugate was obtained as green powder (quantitative).

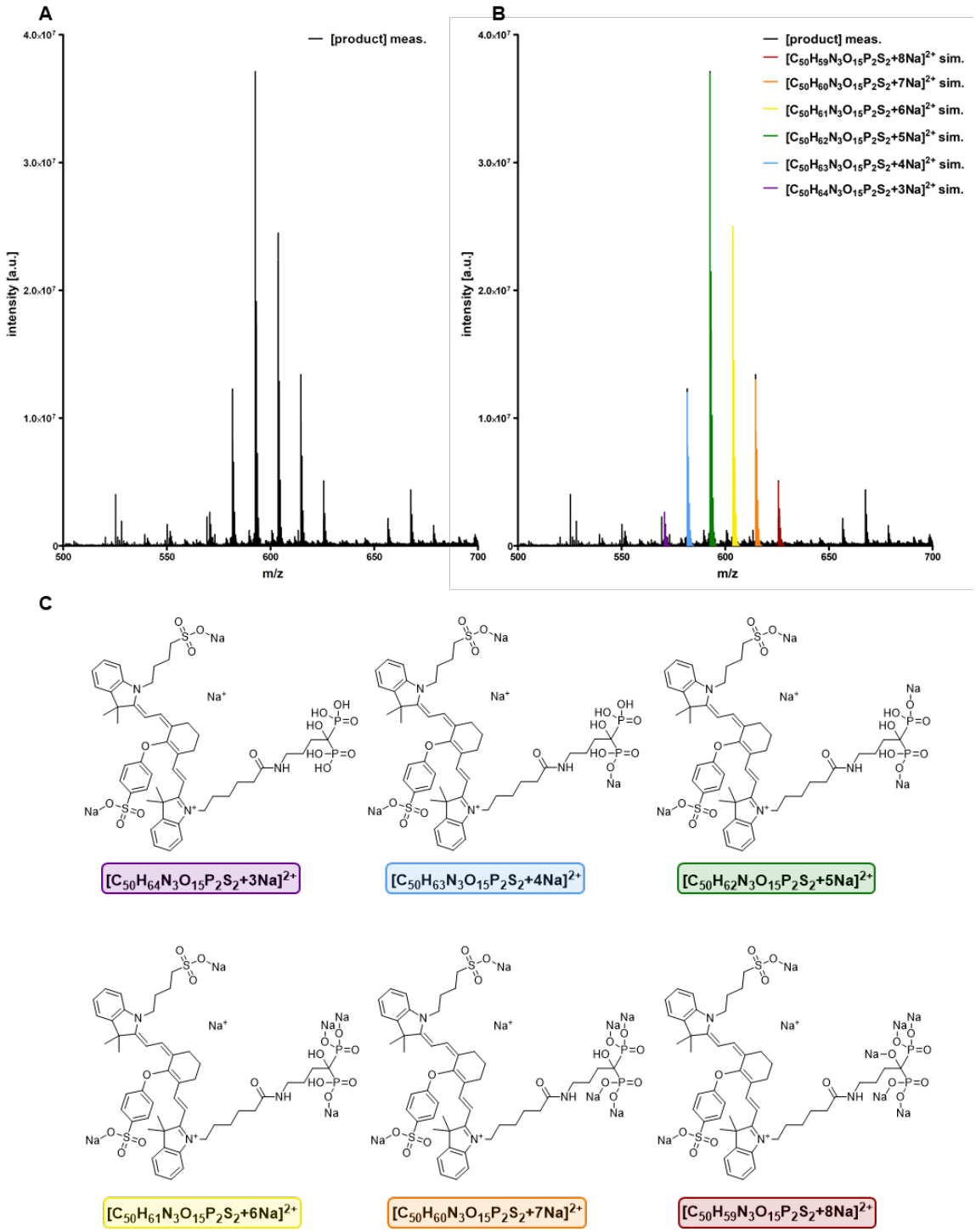

Fig. S6: (A) ESI-MS spectrum of 800RS-labeled alendronate (NIR-AL), (B) ESI-MS spectrum of NIR-AL overlayed with simulated ESI-MS spectrum of identified ionic species, and (C) their corresponding chemical structures.

3.3 Block Copolymer Synthesis

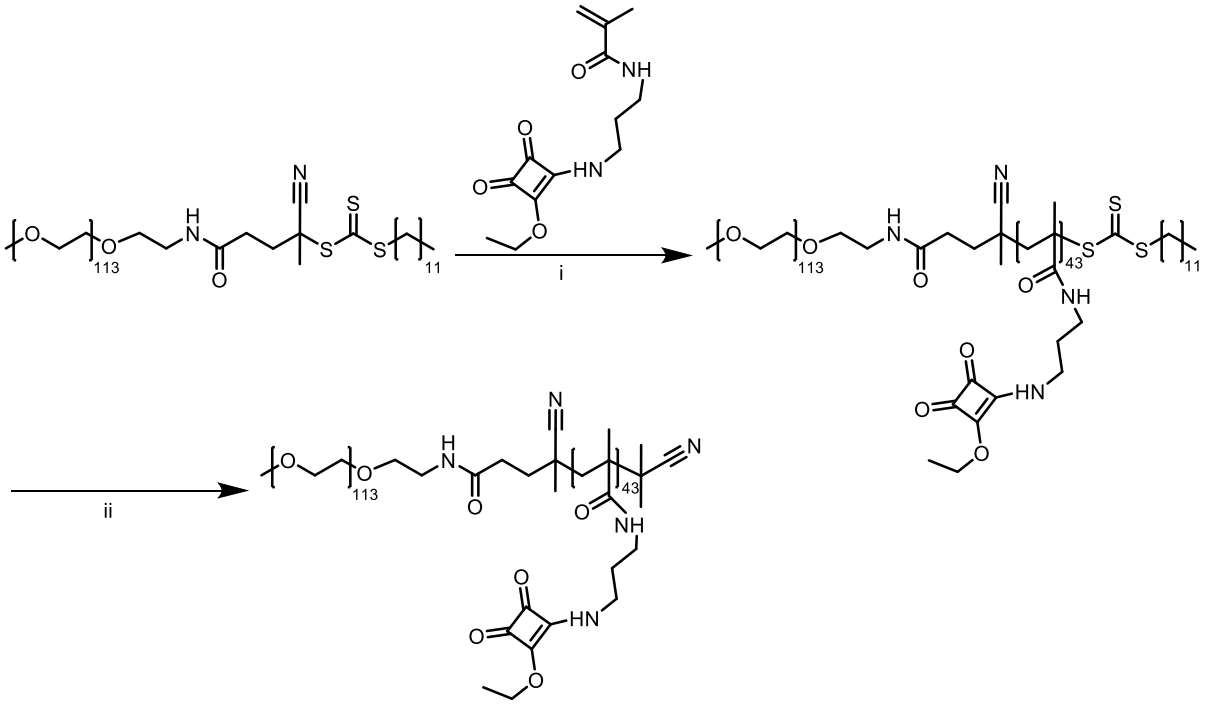

Fig. S7: Synthesis of block copolymer $mPEG_{113}$-(p(MA-SQ)$_{43}$ with macro-PEG-DDC-TTC-CTA, i) AIBN, DMF, 70 °C, 42 h, yield: quantitative, ii) excess AIBN, DMF, 70 °C, 12 h, yield: quantitative %.

As recently described by Huppertsberg et al. amphiphilic poly(ethylene glycol)-b-poly(N-(3-(2-ethoxy-3,4-dioxocyclobut-1-en-1-yl)amino)propyl)-methacrylamide ($mPEG_{113}$-p(MA-SQ)$_{43}$) block copolymers were prepared by reversible addition-fragmentation transfer (RAFT) polymerization of N-(3-(2-ethoxy-3,4-dioxocyclobut-1-en-1-yl)amino)propyl)methacrylamide (MA-SQ) using $mPEG_{113}$-dodecyl-trithiocarbonate-CTA as macro-CTA, whose syntheses were described in detail as well (2).

Block Copolymerization (i)

In a typical block copolymerization AIBN (1.3 mg, 8.0 µmol, 0.2 eq.), macro-CTA (200.0 mg, 40.0 µmol, 1.0 eq.), and MA-SQ (533.0 mg, 2.0 mmol, 50 eq.) were loaded into a Schlenk tube equipped with a stirring bar and dissolved in anhydrous DMF (2 mL). After three freeze-pump-thaw cycles the reaction mixture was placed into an oil bath at 70 °C for 42 h, while being in its evacuated state. After the reaction time,[1] H-NMR analysis of a reaction mixture aliquot indicated a monomer conversion of 86 %. The block copolymer was isolated by three-fold precipitation in cold diethyl ether (-20 °C) and subsequent centrifugation. Drying under high vacuum for 12 h afforded $mPEG_{113}$-p(SQ-MA)$_{43}$-CTA (734.8 mg, 44.5 µmol, quantitative) as yellow solid.

SEC (HFIP, PMMA-Std.): M_n = 37,600 g/mol, M_w = 41,330 g/mol, PDI =1.10.

End group removal (ii)

To remove the trithiocarbonate end group of the block copolymer $mPEG_{113}$-p(MA-SQ)$_{43}$-CTA (720.0 mg, 43.6 µmol, 1. eq.) and AIBN (358.0 mg, 2.20 mmol, 50 eq.) were dissolved under an inert argon atmosphere in anhydrous DMF (3 mL) in a Schlenk tube equipped with a stirring bar. The reaction mixture was immersed in an oil bath at 70 °C for 16 h, before the block copolymer was purified by three-fold precipitation into cold diethyl ether and centrifugation. Finally, the polymer was dried under high vacuum for 14 h affording $mPEG_{113}$-p(MA-SQ)$_{43}$ (570 mg, 34.5 µmol, 79 %) as yellow solid.

^{1}H-NMR (300 MHz, DMSO-*d*$_6$): δ (ppm) = 8.74 (s, 0.5H, **a**)[a)], 8.58 (s, 0.5H, **a**)[a)], 7.31 (s, 1H, **b**), 4.76-4.54 (m, 2H, **c**),3.83-3.48 (m,10H, **d**), 3.48-3.35 (m, 1H, **e**)[a)], 3.30-3.17 (m, 1H, **e**)[a)], 3.17-2.74 (m, 2H, **f**), 1.92-0.48 (m, 10H, **g**). [a)]due to rotamers a splitting of the signals is observed.

SEC (HFIP, PMMA-Std.): M_n = 37,050 g/mol, M_w = 40,310 g/mol, PDI =1.09.

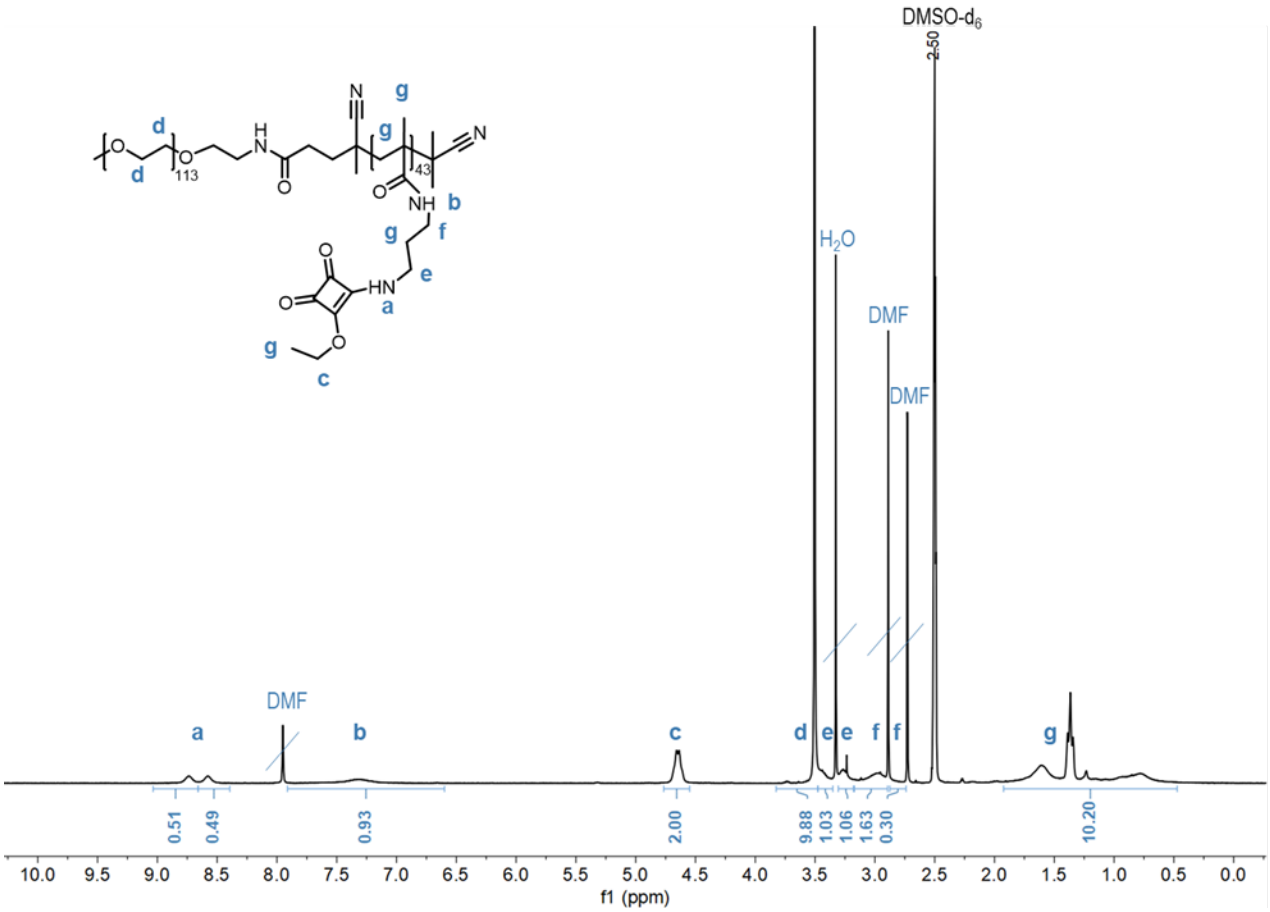

Fig. S8: ^{1}H-NMR (300 MHz) spectrum of mPEG$_{113}$-p(SQ-MA)$_{43}$ in DMSO-d$_6$.

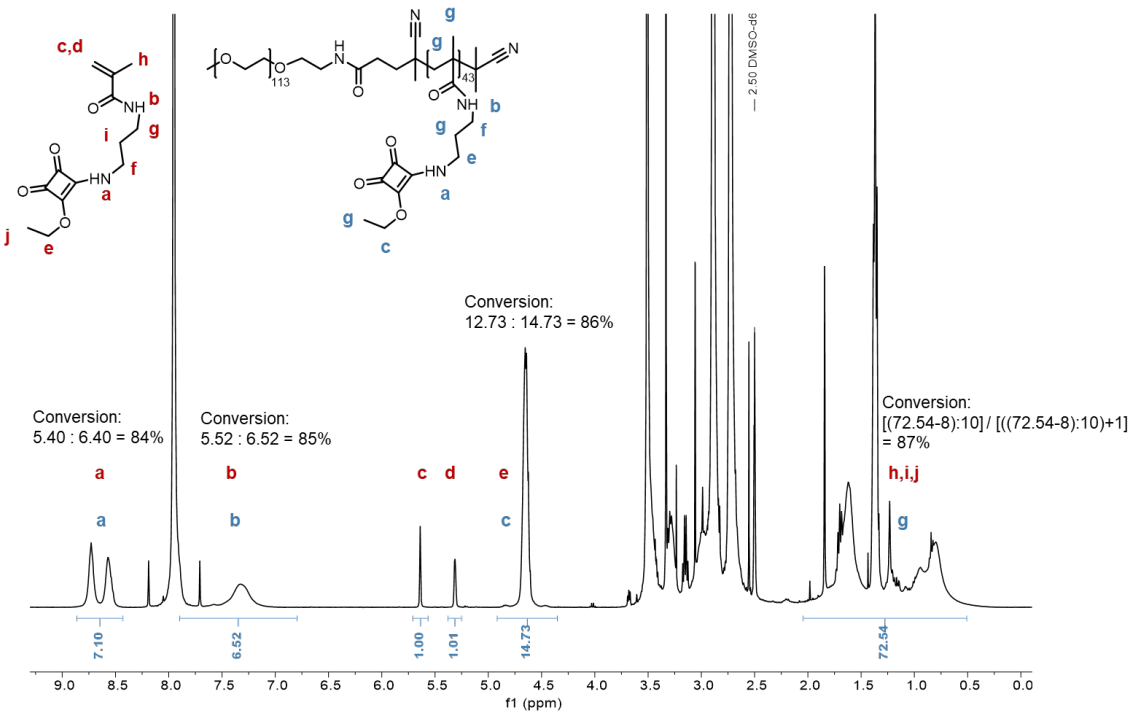

Fig. S9: ^{1}H-NMR (300 MHz) spectrum of reaction mixture of mPEG$_{113}$-p(SQ-MA)$_{43}$-CTA in DMSO-d$_6$. From the averaged conversion a DP of 43 was calculated.

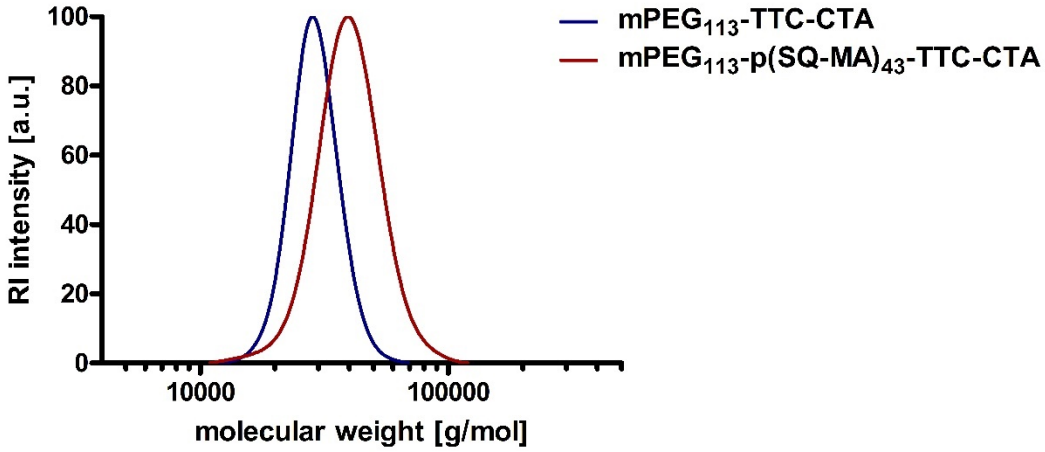

Fig. S10: HFIP SEC elugram of the macro chain transfer agent (mPEG$_{113}$-TTC-CTA) (blue) and the corresponding block copolymer mPEG$_{113}$-p(SQ-MA)$_{43}$TTC-CTA before end group removal (red).

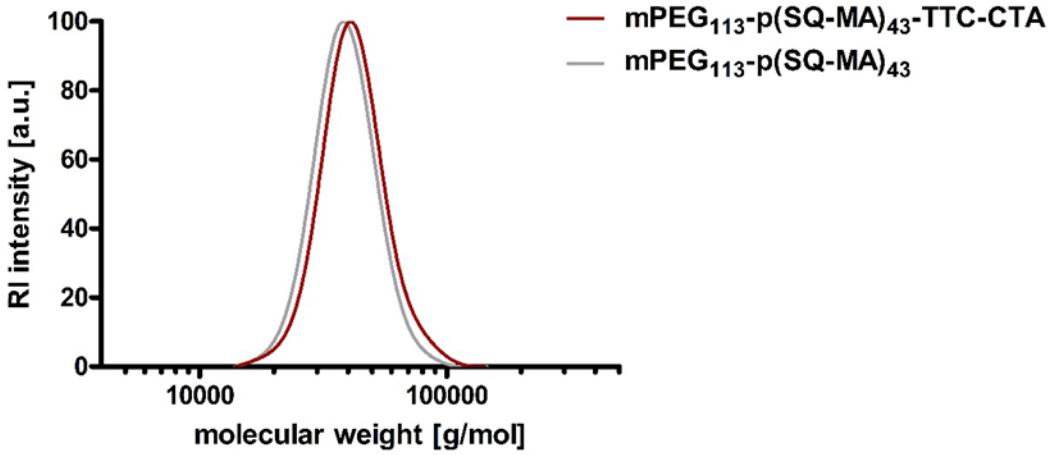

Fig. S11: HFIP SEC elugram of the block copolymer $mPEG_{113}$-p(SQ-$MA)_{43}$ before (red) and after end group removal (grey).

Table S1: Summarized ^{1}H-NMR and SEC data stating the molecular weight, degree of polymerization (DP), and polydispersity index (PDI) of $mPEG_{113}$-TTC-CTA as well as the corresponding block copolymer with and without end group ($mPEG_{113}$-TTC-p(SQ-$MA)_{43}$-CTA and $mPEG_{113}$-TTC-p(SQ-$MA)_{43}$. DP was calculated by ^{1}H-NMR spectroscopy from the crude reaction mixture.

polymer	^{1}H NMR		SEC		
	M [g/mol]	DP	M_N [g/mol]	M_W [g/mol]	PDI
$mPEG_{113}$-TTC-CTA	5,440	-	28,110	29,610	1.05
$mPEG_{113}$-p(SQ-$MA)_{43}$-TTC-CTA	16,890	43	37,600	41,330	1.10
$mPEG_{113}$-p(SQ-$MA)_{43}$	16,680	45	37,050	40,310	1.09

3.4 Nanogel Synthesis

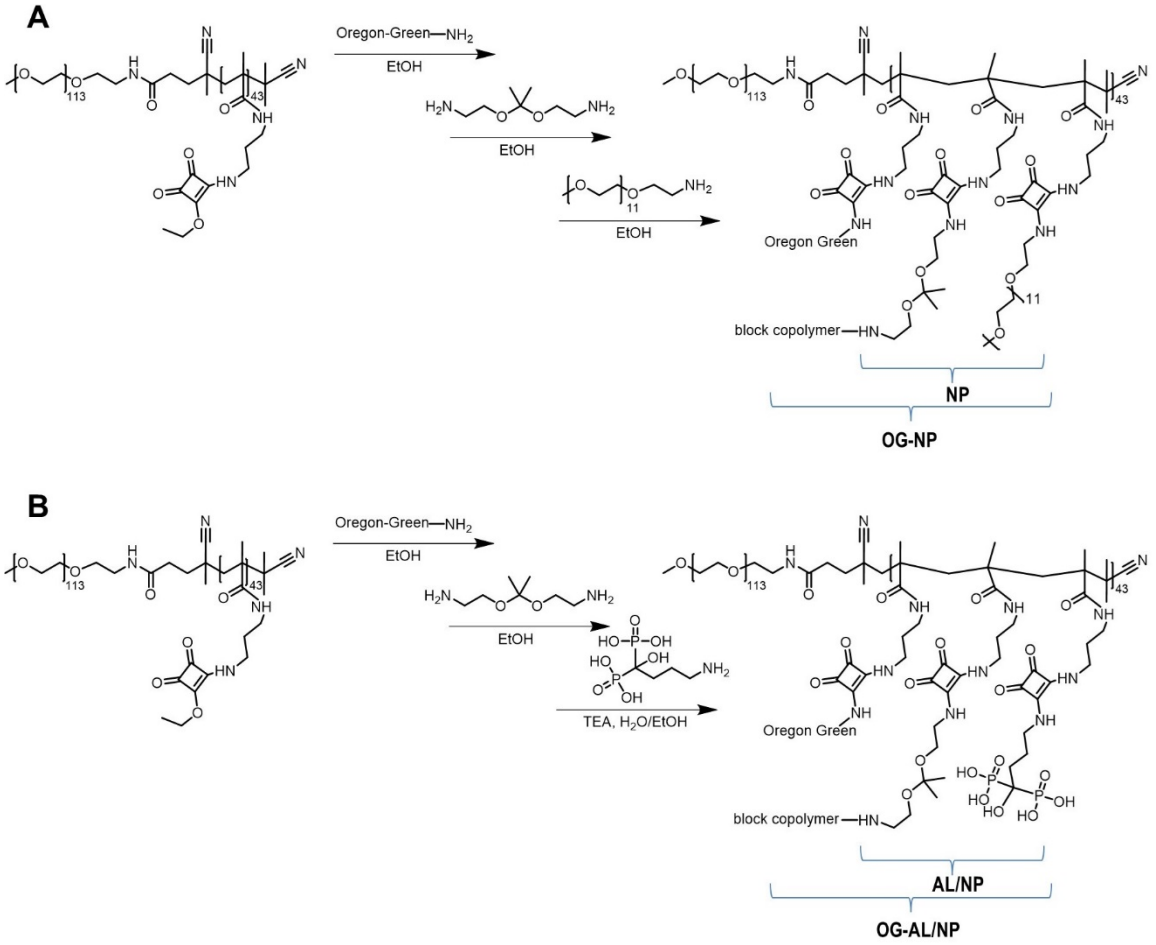

Fig. S12: Scheme of sequential preparation of nanogels without drug load (NP, and OG-NP) and with drug load (AL/NP, and OG-AL/NP).

The synthesis of nanogels derived from $mPEG_{113}$-$p(SQ\text{-}MA)_{43}$ has been described earlier. (2)
The preparation of pH-responsive alendronate-loaded nanogels (AL/NP) as well as control nanogels without drug load (NP) was proceeded in analogy and is described in detail in the following.
Polymeric micelles were prepared by dispersion of the block copolymer $mPEG_{113}$-$p(SQ\text{-}MA)_{43}$ (116 mg, 7.02 µmol polymer, 302.24 µmol reactive squaric ester amide units) in ethanol at a final concentration of 10 mg/mL. After 1 h ultrasonication DLS measurements of the dispersion verified the self-assembly of polymeric micelles.
To prepare pH-responsive crosslinked nanogels with and without dye-labeling the micellar dispersion was divided into two. Therefore, 6.0 mL (60.0 mg, 3.78 µmol polymer, 151.12 µmol reactive squaric ester amide units) was transferred into two Schlenk tubes equipped with stirring bar, respectively. For fluorescent labeling of the nanogels 150 µL of Oregon Green dye stock solution (2.5 mg/mL in DMSO, 375.14 µg, 0.76 µmol, 0.005 eq.) as well as ketal-containing crosslinker 2,2-bis(aminoethoxy)propane (3.6 µL, 22.6 µmol, 0.15 eq.) was added to one half, whereas to the other half only the crosslinker was added. The reaction mixtures were stirred at RT for two days, before the dye-labeled and native crosslinked micelles were used to prepare drug-loaded as well non-drug-loaded nanogels. Instead of the immune-modulating bisphosphonate alendronate, the latter were conjugated with $mPEG_{11}$ -NH_2.

Thus, both dispersions were divided into two, wherefore 3 mL (30.0 mg, 1.89 µmol polymer, 75.56 µmol reactive squaric ester amide units) of each dispersion was transferred into two Schlenk tubes, respectively yielding a total of four dispersions.
For preparation of control nanogels without drug load, an excess of $mPEG_{11}$-NH_2 stock solution (2 mL, 85 mg/mL in DMSO, 226.69 µmol, 170.01 mg, 3 eq.) was added to one dye-labeled as well as one native dispersion. To fabricate alendronate-loaded nanogels, an excess of alendronate stock solution (4.46 mL, 27.58 mg/mL in milliQ-H_2O, 377.81 µmol, 123.0 mg, 5 eq. with 0.263 mL TEA (1.89 mmol, 191.15 mg, 25 eq.)) was added to the remaining dye-labeled and native dispersions. The total of four dispersions was allowed to stir for another seven days. Complete conversion of the reactive ester units was confirmed by UV-Vis absorbance measurements.
To remove small molecular byproducts, the dispersions were purified by dialysis (MWCO: 1 kDa) against milliQ-H_2O containing 0.1 % NH_3 (1 L) for seven days with water exchange twice per day. After subsequent lyophilization the alendronate-loaded nanogels (OG-AL/NP, AL/NP) were obtained as orange or slightly yellowish powder (39 mg and 41 mg), whereas the PEG-loaded nanogels (OG-NP, NP) were afforded as orange or white powder (56 and 55 mg).
For *in vivo* experiments, the nanogels were labeled with the NIR dye 800RS cadaverine. Nanogel preparation was proceeded in analogy with the variation that 560 µL of 800RS cadaverine dye stock solution (2.5 mg/mL in DMSO, 1.4 mg, 1.51 µmol, 0.01 eq.) was added for fluorescent labeling. The nanogels (NIR-NP and NIR-AL/NP) were obtained as green powder (30 and 31 mg).

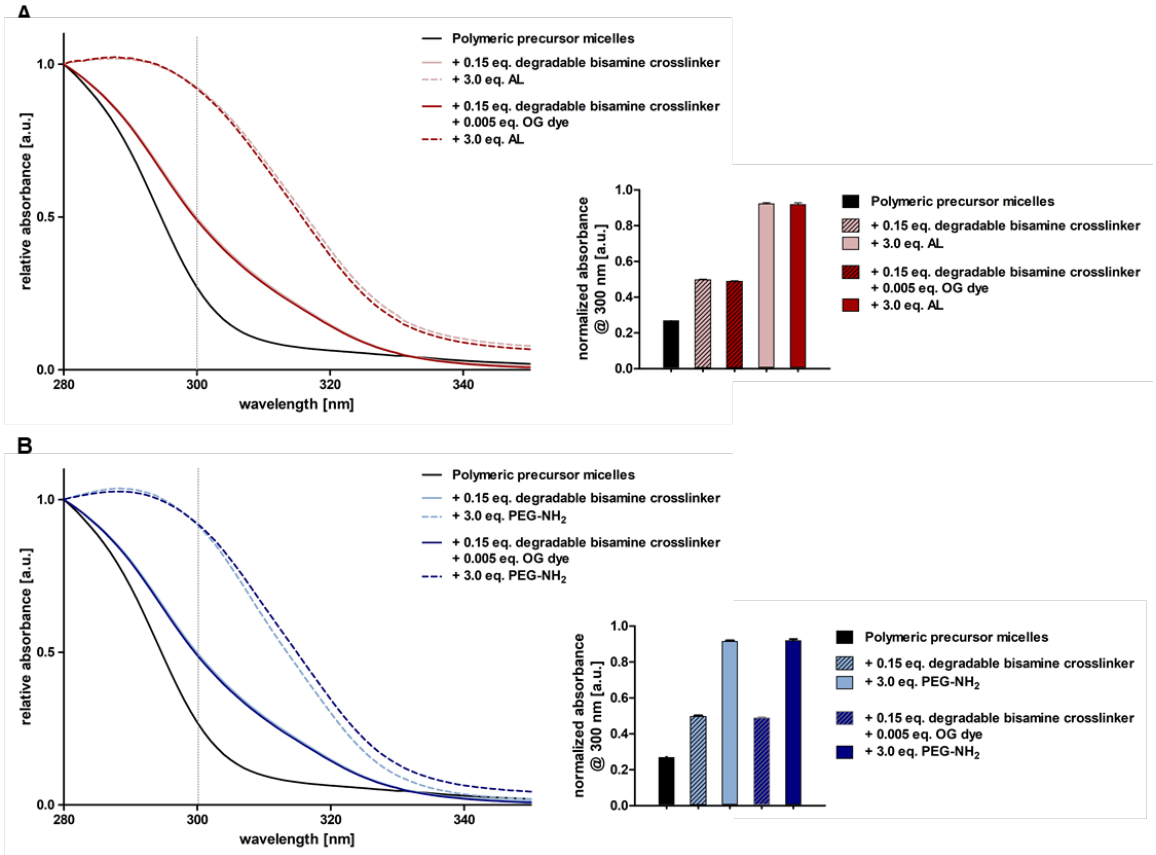

Fig. S13: Conversion of polymeric squaric ester amides to squaric bisamides during nanogel synthesis of AL/NP and OG-AL/NP (A) as well as of PEG/NP and OG-PEG/NP (B) monitored by UV absorbance. UV-Vis spectra of polymeric precursor micelles after sequential addition of OG dye, degradable crosslinker, and AL or PEG-NH_2 show a step-wise increase in the absorbance around 300 nm corresponding to squaric bisamide formation.

4. Nanogel Characterization

4.1 Dynamic Light Scattering (DLS)

Single-angle DLS measurements of alendronate-loaded as well as empty nanogels (AL/NP, NP) with or without fluorescent Oregon Green labeling (AL/NP, NP, OG-AL/NP, OG-NP) were performed at 25 °C using a Malvern ZetaSizer Nano S purchased from Malvern Instruments Ltd (Malvern, Great Britain) with a He/Ne Laser (λ = 633 nm) at a fixed scattering angle of 173°. All measurements were performed in triplicate. Data is given as mean of three repeated measurements per sample. The obtained data was processed by cumulant fitting for z-average and PDI, or by CONTIN fitting for intensity-, volume-, and number-weighted particle size distribution. Unless stated otherwise, samples were prepared at 2 mg/mL in PBS. Dust was removed prior to each measurement by filtration through GHP syringe filters (0.2 µm pore size, Acrodisc).

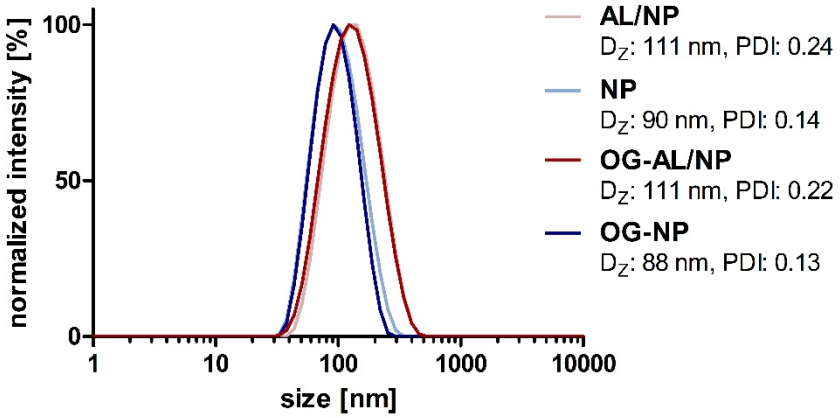

Fig. S14: Intensity-weighted DLS size distribution of AL/NP, NP, OG-AL/NP, and OG-NP**.**

4.2 Zeta Potential

Zeta potential was measured using a Malvern Zetasizer Nano ZS purchased from Malvern Instruments Ltd (Malvern, Great Britain). The samples were prepared at 0.5 g/mL in HEPES buffer (pH 7.4) and transferred into folded capillary zeta cells (DTS 1070). The zeta potential was determined by applying the Smoluchowski equation. All measurements were performed in triplicate. Data is given as mean of three repeated measurements per sample.

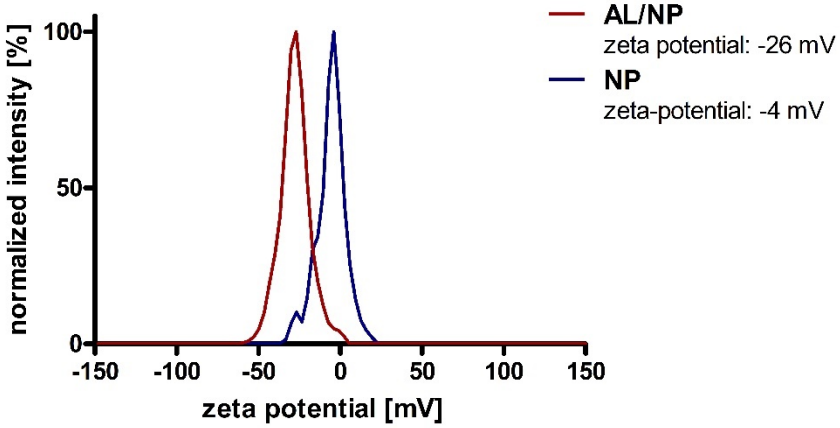

Fig. S15: Zeta potential measurements of AL/NP and NP.

4.3 Nanogel Disassembly Studies via Dynamic Light Scattering

The pH-responsive disassembly of the nanogels was investigated by DLS. Therefore, the lyophilized nanogels were re-dispersed in acidic 50 mM acetate buffer (pH 5.4) at a concentration of 2 mg/mL, followed by five minutes intense vortexing. Subsequently DLS measurements were performed directly (5 min) and after 24 h.

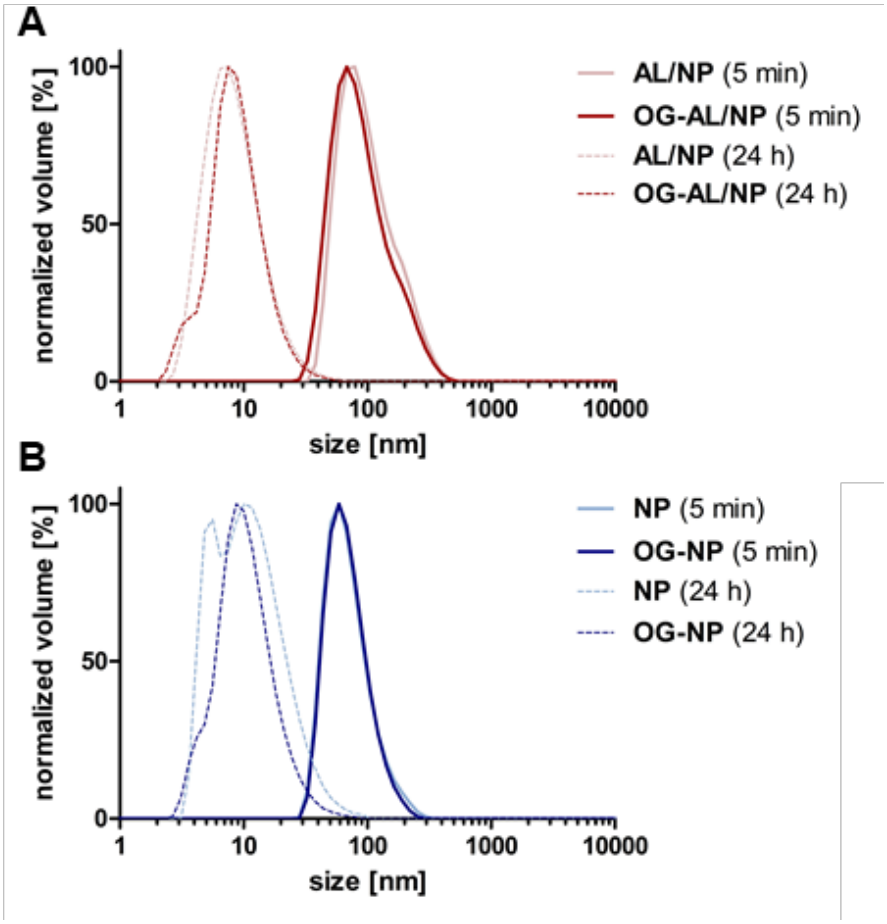

Fig. S16: DLS degradation study of AL/NP (A) as well as NP (B) with or without fluorescent Oregon Green (OG-) labeling under acidic conditions (pH 5.4).

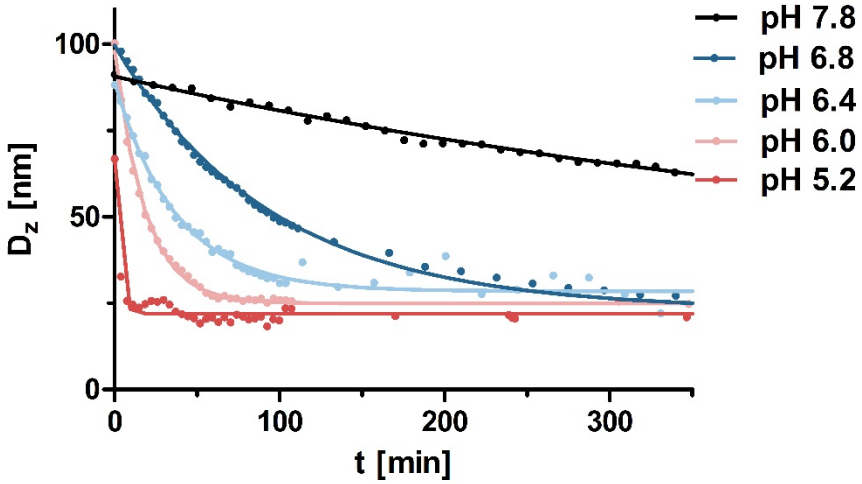

Fig. S17: DLS z-average (D_z) of AL/NP upon exposure to pH value 7.8 compared to mildly acidic pH values of 6.8, 6.4, 6.0, and 5.2 over time indicating that the installed pH-sensitivity results in nanogel degradation.

4.4 Quantification of Alendronate Drug Load in AL/NP

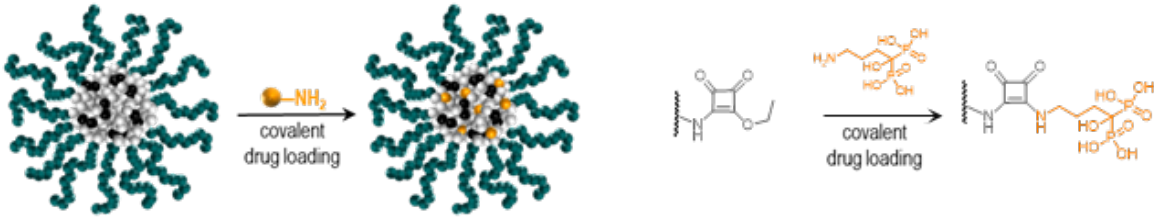

Fig. S18: Scheme of covalent drug loading of alendronate to nanogel core through reaction of alendronate's amino group with the pendant squaric ester group in the micellar core.

Determination by ^{31}P NMR

Since the bisphosphonate alendronate bears two ^{31}P atoms, whose nuclei are NMR active, the drug load of the alendronate-loaded nanoparticles (AL/NP, OG-AL/NP) was determined by ^{31}P NMR.

For this purpose, initially a D_2O stock solution (13 mL with 0.1 vol% NH_3) as well as KH_2PO_4 (10 mg/mL) as internal standard was prepared. Next, this stock solution was used to prepare several alendronate standards in the range of 0, 0.75, 1.25, 2.5, 5, and 10 mg/mL. From the corresponding ^{31}P NMR spectra it was evident that alendronate followed strong linear correlation in the given concentration range.

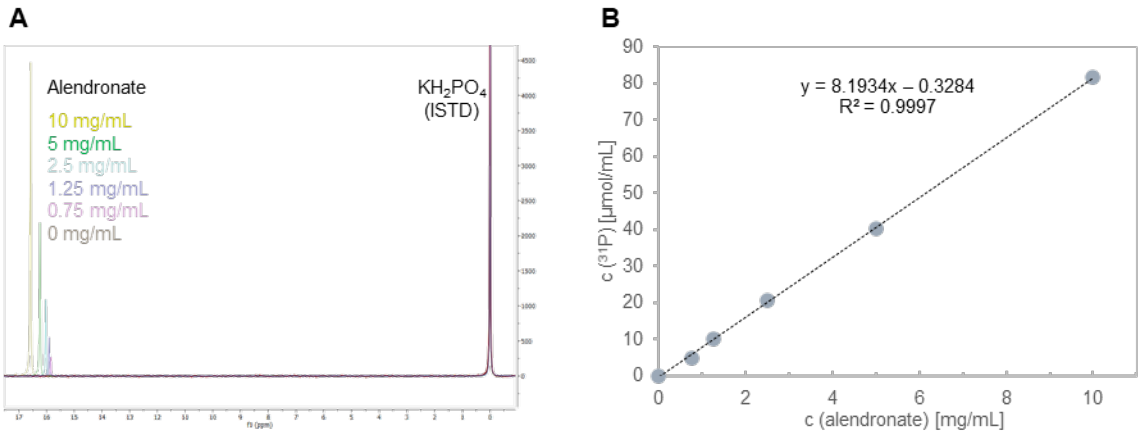

Fig. S19: Overlayed ^{31}P NMR spectra of Alendronate standards (0-10 mg/mL in D_2O with KH_2PO_4) (A) and the corresponding linear regression function (B).

AL/NP and OG-AL/NP were dissolved in the same D_2O stock solution containing 10 mg/mL KH_2PO_4 at a final concentration of 10 mg/mL and ^{31}P NMR spectra were recorded. Based on the ratio between the integral of ISTD and alendronate the drug load of the NP was calculated.

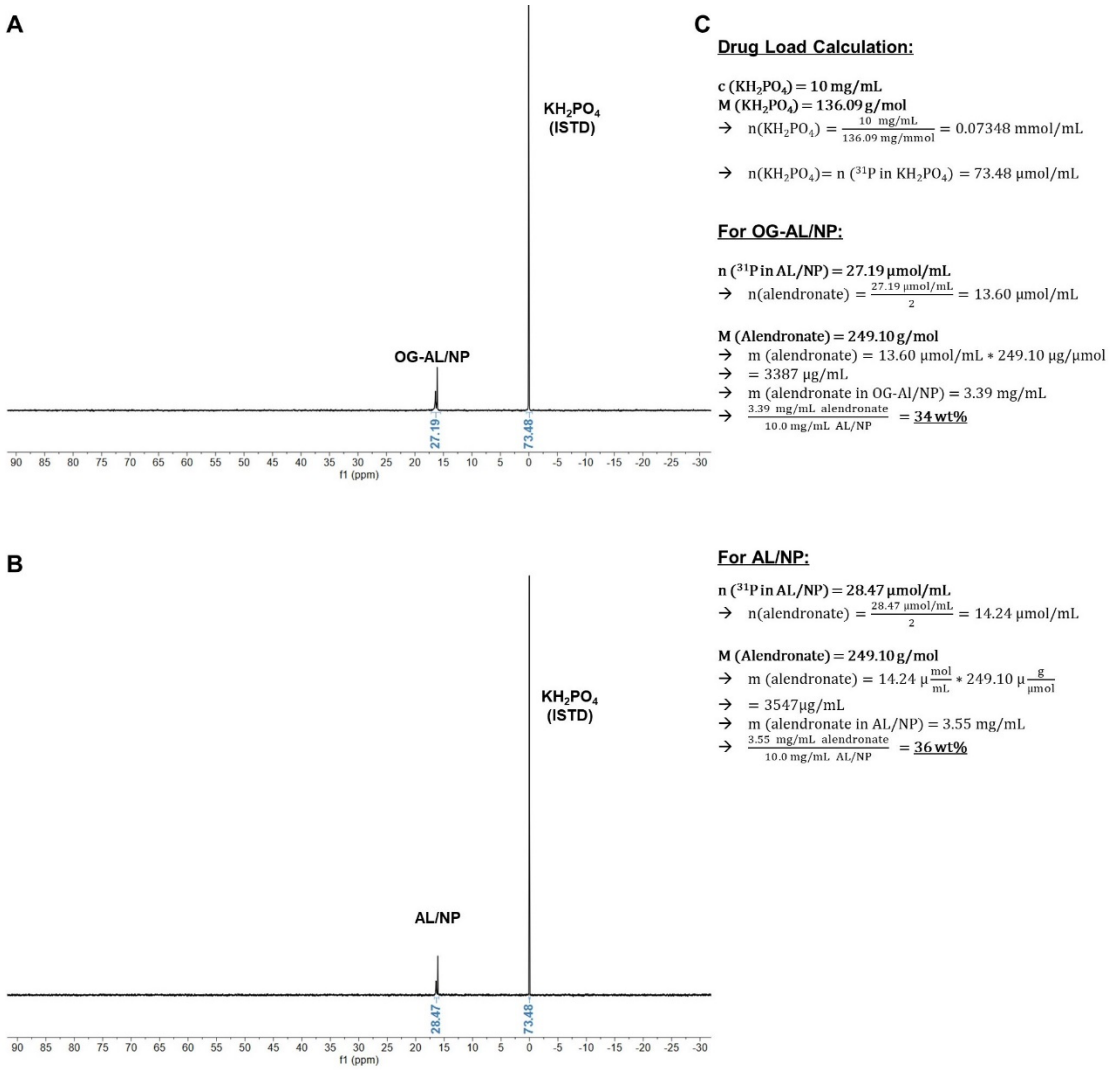

Fig. S20: Alendronate load quantification by ^{31}P NMR: ^{31}P NMR spectra of OG-AL/NP (A) and AL-NP (B) at a concentration of 10 mg/mL in D_2O with KH_2PO_4, as well as the corresponding drug load calculations resulting from the obtained integrals (C).

Colorimetric determination of orthophosphate by Molybdenum Blue Method

In addition to the drug load determination by ^{31}P NMR analysis, the NP's alendronate load was confirmed by spectrophotometric determination using the molybdenum blue method.

For this purpose, a 1 mg/mL alendronate stock solution was prepared, from which several alendronate standards in the range of 0, 2.5, 5.0, 7.5, 10, 12.5, and 15 µg/15 µL (0, 0.17, 0.33, 0.5, 0.67, 0.83, 1.0 mg/mL) were prepared in water. NP samples (AL/NP, and NP) were prepared at 1 mg/mL in water.

For chemical oxidation of the bisphosphonate alendronate to orthophosphate 50 µL of oxidizing ammonium persulfate ($(NH_4)_2S_2O_8$) stock solution (10 mg/mL in H_2O) was added to each standard and NP sample. These reaction mixtures were heated up to 90 °C for 10 min. After they were cooled down using an ice bath, 700 µL of 0.45 wt% ammonium molybdate tetrahydrate ($(NH_4)_6Mo_7O_{24}\cdot 4H_2O$) and 700 µL of 1.7 wt% ascorbic acid stock solution were added and the reaction mixtures were heated up to 60 °C for 3 min. The absorbance of the thereby formed molybdenum blue species, which is proportional to alendronate, was recorded by UV Vis absorbance (A_{max} = 855 nm).

From the corresponding absorbance spectra of the alendronate standards or more specifically their absorbance at 855 nm the linear correlation function could be given. To calculate the alendronate

drug of the NP samples, the absorbance at 855 nm of the “blank” NP sample was subtracted from the absorbance measured at 855 nm for the respective AL/NP sample. By inserting these values into the determined linear correlation function the AL-load could be calculated.

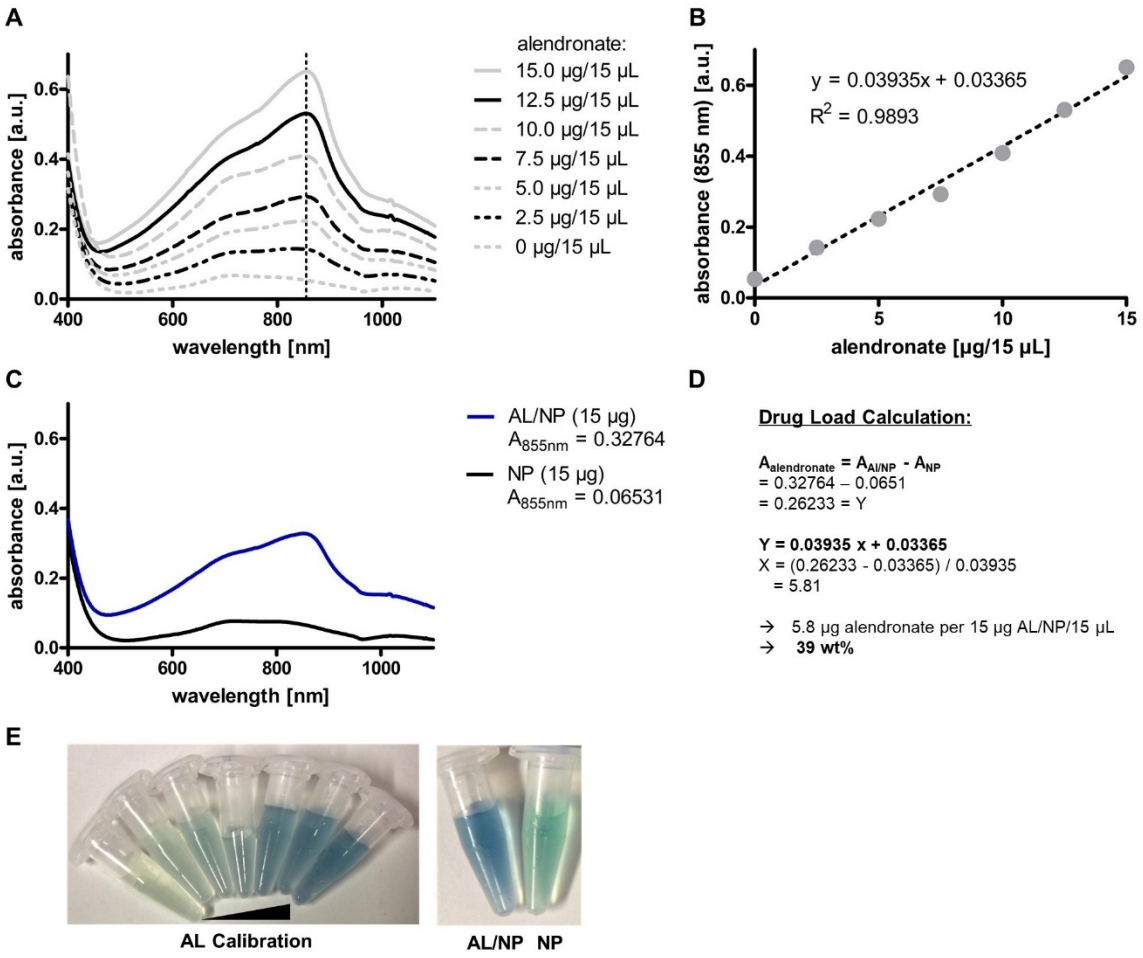

Fig. S21: Alendronate load quantification by photometric molybdenum blue assay. (A) Overlayed UV-Vis absorbance spectra of alendronate standards (0-15 µg/15 µL), (B) linear correlation function for their corresponding absorbance at 855 nm, (C) absorbance spectra of AL/NP and empty NP, (D) drug load calculations, (E) and photographs of alendronate calibration standards and NP samples.

4.5 Stability Study in human plasma via Dynamic Light Scattering

To evaluate the stability of the alendronate-loaded and PEG-loaded nanoparticles in plasma DLS experiments were performed after plasma incubation. Therefore, 50 µL particle dispersion (20 mg/mL) was diluted with 1 mL plasma and incubated at 37 °C for 1 h. Subsequent DLS measurements were carried out with a Uniphase He/Ne Laser (632.8 nm, 22 mW), an ALV-SP125 Goniometer, an ALV/High QE APD-Avalanche photodiode, an ALV5000/E/PCI-correlator and a Lauda RC-6 thermostat unit. The angular dependent measurements were performed between 30° and 150° in 20° steps. Data analysis was performed according to the procedure described by Rausch et al.(3)

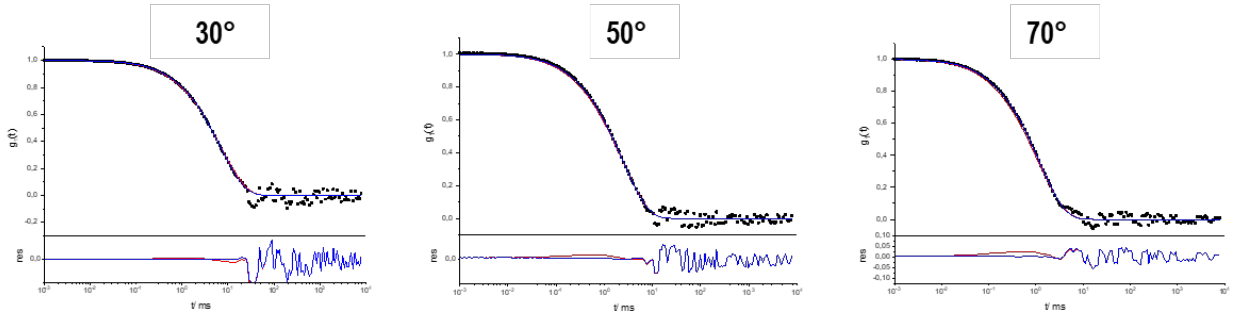

Fig. S22: DLS Study of OG-AL/NP after plasma incubation. Upper graphs show autocorrelation functions g1(t) (black dots) of the NP/plasma mixture at scattering angles of 30°, 50°, or 70°. The fit of the sum of the individual components is displayed by the red line, whereas the blue line represents the fit including an additional aggregation function. Lower graphs display the residuals which result from the difference between data and the two fits.

4.6 Stability Study in human plasma via Fluorescence Correlation Spectroscopy

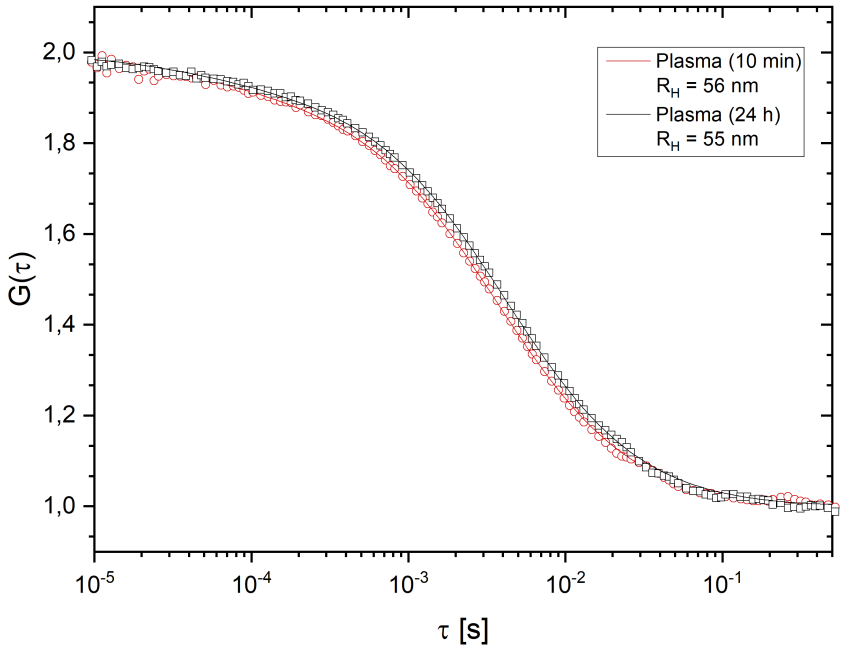

Fig. S23: FCS study of OG-labeled AL/NP after human blood plasma incubation. Normalized autocorrelation curves (dots) and corresponding fits (solid line) after plasma incubation for 10 min, and 24 h.

4.7 UV-Vis Absorbance and Fluorescence Spectroscopy Characterization

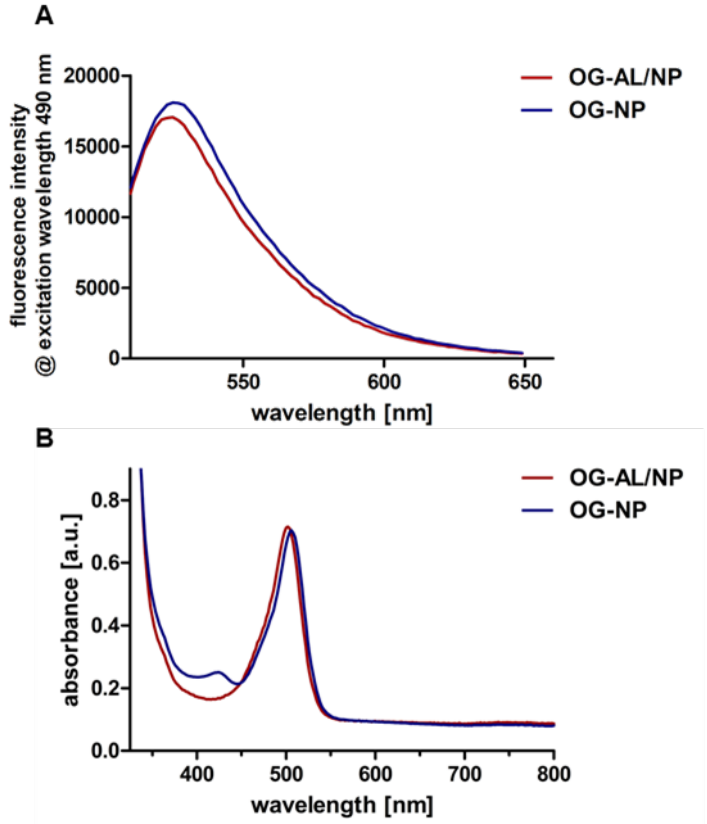

Fig. S24: (A) Fluorescence intensity and (B) UV-Vis absorbance spectrum of OG-AL/NP and OG-NP at 2 mg/mL.

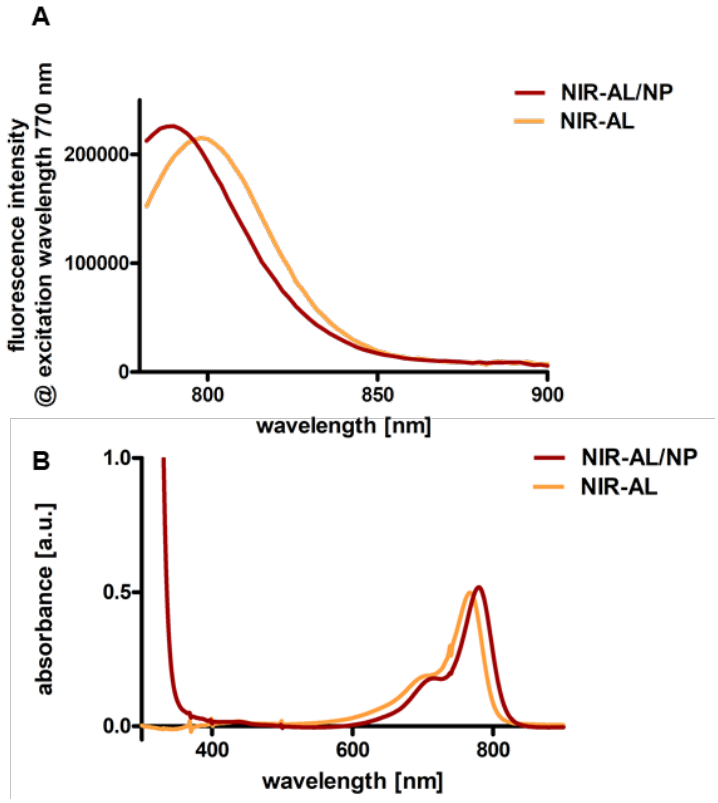

Fig. S25: A) Fluorescence intensity and (B) UV-Vis absorbance spectrum of NIR-AL/NP and NIR-AL at 2 mg/mL.

5. *In Vitro* Studies

5.1 Cell culture

RAW 264.7 macrophages were cultured in Dulbecco's modified Eagle's medium (Sigma-Aldrich, Taufkirchen, Germany) supplemented with 10% fetal bovine serum (FBS), 1% penicillin/streptomycin, 1% L-glutamine in 5% CO_2 at 37°C. The medium was routinely changed every 2 days and the cells were separated by cell scraping before reaching confluency. As *in vitro* model for hepatic macrophages, myeloid precursor cells were harvested from bone marrow of mice and differentiated in the presence of macrophage colony-stimulating factor (M-CSF, ImmunoTools, Germany), a lineage-specific growth factor, into primary macrophages. Once matured to macrophages, they exert numerous phenotypic characteristics of monocyte-derived macrophages. They exhibit an elevated expression of CD206 (macrophage mannose receptor) when polarized towards M2 (compare Fig. 4B in (4)), while M1-type macrophages, as the anti-fibrotic phenotype, and native M0 macrophages are characterized by an expression of CD206, respectively. Thus, primary macrophages are an ideal cell model to mirror characteristics of liver resident macrophages *in vitro*.

Primary bone marrow derived macrophages (BMDM) were harvested from 6-9 weeks old BALB/c mice as described by us in detail before (4, 5). In brief, mice were sacrificed by cervical dislocation, and femurs and tibias were isolated under sterile conditions. A 21G needle and a 10 mL syringe were used to flush out the marrow into cold PBS substituted with 2% heat inactivated FBS and 1% penicillin/streptomycin. Subsequently, single cell suspensions were passed through a 70 µm cell strainer to exclude cell clumps and other impurities. Contaminating erythrocytes were removed with red cell lysis buffer (eBioscience, USA, SanDiego). Cells were resuspended in Iscove's Modified Dulbecco's Medium (IMDM), 10% FBS, 1% penicillin/streptomycin, 1% L-glutamine containing 25 ng/mL monocyte-colony stimulating factor (M-CSF, ImmunoTools, Germany, Friesoythe). 5 million BMDM in 10 mL media were seeded into bacterial culture plate (Sigmal-Aldrich/Merck, Darmstadt, Germany), to facilitate better detachment and improved viability of the cells during passaging. On day 3, half of the media in the petri dishes was replaced with fresh IMDM containing the same supplements. Immature BMDM were incubated for additional 4 days with M-CSF for further differentiation into mature primary macrophages. For polarization towards an M2- or M1-phenotype, primary macrophages were incubated with fully supplemented IMDM containing 20 ng/mL interleukin 4 and 13, or 50 ng/mL interferon γ and 0.1 µg/mL LPS (all from ImmunoTools), respectively, for 24 h. For subculturing and cell harvest, cells were preincubated in PBS (phosphate buffered saline - calcium and magnesium free), supplemented with 10 mM EDTA, for 15 min on ice and subsequently gently detached by cell scraping.

5.2 In Vitro Cytotoxicity

The MTT (3-(4,5-dimethylthiazol-2-yl)-2,5-diphenyltetrazolium-bromide) or alamarBlue assay was used to assess the cytotoxic effects of AL/NP, AL and unloaded carrier (NP) on RAW-macrophages as described before (4–7). In brief, cells were seeded into 96-well plates at a density of approximately 6000-7000 cells per well and incubated in supplement containing medium. RAW-macrophages were polarized for M1- and M2-type as described above. For native macrophages (M0-type) equal amounts of PBS were added. After 24 h of polarization or incubation, respectively, increasing concentrations of AL/NP (corresponding to 5, 10, 20, 100, 250, 500, 1000 nM AL were added. After 48 h of incubation, 20 µL of MTT in PBS (4 mg/mL) was added to the culture medium and incubation was carried out for another 5 h. Afterwards, the medium was carefully removed and 150 µL DMSO was added. Plates were placed on an orbital shaker for 1 h under exclusion of light for homogenization. Finally, the OD at 570 nm were measured on an Infinite M200Pro spectrofluorometer (TECAN, Männerdorf, Switzerland). As reference the OD570 of nanoparticle-treated cells was normalized by the OD570 of cells exposed to equal volumes of PBS alone.

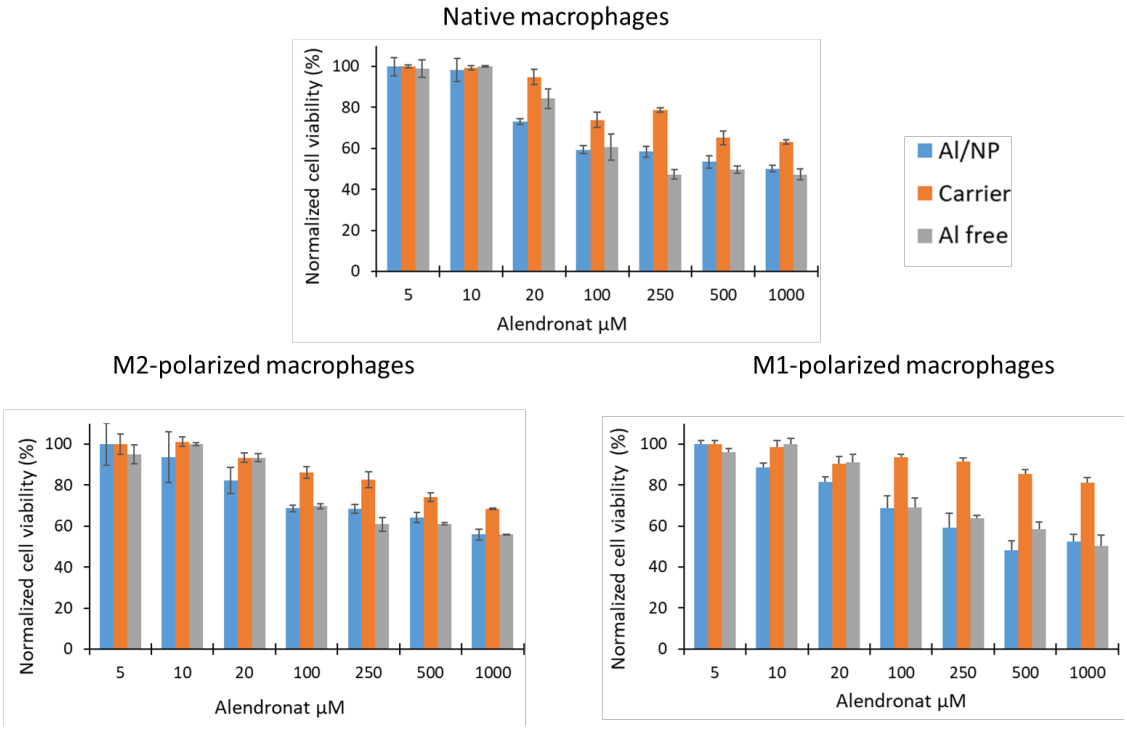

Fig. S26: *In vitro* cytotoxicity of AL/NP and controls (AL, NP) in native, M1, and M2 polarized primary macrophages as determined by MTT assay (N=3). Cell toxicity was related rather to the drug (AL) than the carrier (NP) itself.

5.3 In Vitro Effect of AL/NP

Primary macrophages were seeded into 6-well plates at a density of 350.000 cells per well and polarized towards a M2-type as described above. After 24 h polarization, M2-type macrophages were incubated with AL/NP (corresponding to 30 or 60 µM AL), corresponding controls (AL, NP), or equal amounts of PBS for M2-type controls for 48 h. Afterwards, cells were further processed for qPCR- and FACS-analysis as described below.

5.4 Quantitative RT-PCR

Total RNA from cells was isolated directly by guanidinium thiocyanate-phenol- chloroform extraction, while RNA from livers was obtained by the same extraction method but livers were first homogenized, using Tissue Lyser II (Qiagen, Venlo, Nether lands) as reported before (6, 7). For qPCR, 1 µg of total RNA was reverse-transcribed into cDNA using the qScript cDNA SuperMix (Quantas, Beverly, USA). The following SYBR green primers for IL-10, YM-1 and CCL-2 and β-actin were synthesized by Eurofins (Mannheim, Germany):

β-actin: forward 5′-GGCATTGTTACCAACTGGGACGAC-3′
reverse 5′-CCAGAGGCATACAGGGACAGCACAG-3′

IL-10: forward 5′-GCTCTTACTGACTGGCATGAG-3′
reverse 5′-CGCAGCTCTAGGAGCATGTG-3′

YM-1: forward 5′-AGAAGGGAGTTTCAAACCTGGT-3′
reverse 5′-GTCTTGCTCATGTGTGTAAGTGA-3′

CCL-2: forward 5′-GGCTCAGCCAGATGCAGTTAA -3′
reverse 5′-CCTACTCATTGGGATCATCTTGCT-3′

CD206: forward 5'-AAG GCT ATC CTG GTG GAA GAA-3'
reverse 5'-AGG GAA GGG TCA GTC TGT GTT-3'

SYBR reaction mixtures were purchased from Applied Biosystems (Darmstadt, Germany). Transcript levels of β-actin were used to normalize data and to control for RNA integrity. Samples were amplified by the SYBR technology and analyzed using a Step One Plus sequence amplification system from LifeTechnologies (Darmstadt, Germany). Results were calculated by the ΔΔCT method as reported in detail before (4, 6–8).

5.5 In Vitro Fluorescent Activated Cell Sorting Flowcytometry (FACS)

Primary macrophages were seeded in 6-well culture plates at a density of 700,000 cells per well and allowed to adhere overnight. Cells were polarized with 20 ng/mL interleukin 4 and 13 towards a M2-type for 24 h as described above. For *in vitro* cell uptake, M2-type macrophages were incubated with a final concentration of Oregon Green 488 labeled AL/NP, corresponding to 30 or 60 µM AL, or unloaded NP (corr. to ~60 µM AL), respectively for 24 h. Cells were washed with PBS three times, preincubated with EDTA (10 mM in PBS) for 15 min on ice and carefully detached by scarping. To exclude dead cells, cells were stained with a viability dye (Fixable Viability Dye eFluor® 506, eBioscience) according to the manufacture's protocol. For quantification of interleukin-10, cells were permeabilized, using permeabilization buffer from Biolegend (San Diego, USA), and stained with IL-10-APC antibody (Biolegend, clone JES5-16E3) according to the manufacturer's protocol for intracellular staining. Cells were then fixed with 4% formaldehyde for 15 min at 37 °C and subjected to flow cytometry (BD FACSCanto II, BD Bioscience, Canada, Mississauga) the next day. Compensation was performed by BD FACSDiva software version 7.0 with OneComp eBeads from eBioscience. 10,000-50,000 cells were measured per staining. Further data analysis was carried out using open source Flowing Software 2.5.0 (Perttu Terho, Turku Centre for Biotechnology, Finland). Gating procedure was performed as illustrated in **Fig. S25**.

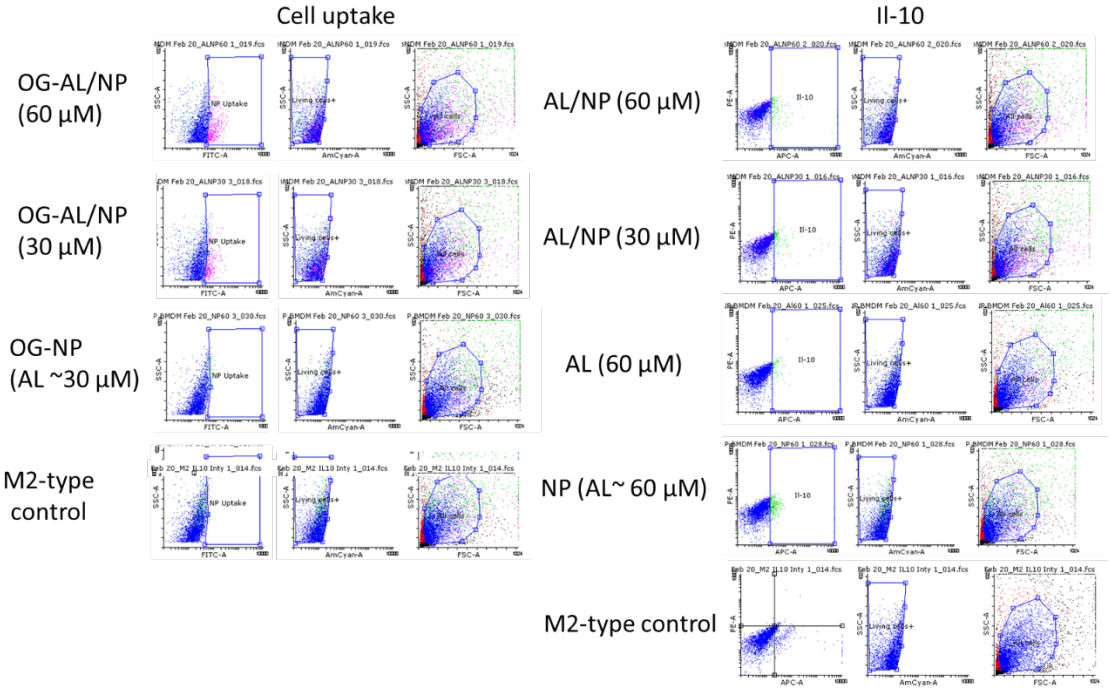

Fig. S27: Exemplary FACS gating procedure to determine the *in vitro* cellular uptake of the OG-AL/NP in M2 macrophages and quantification of Il-10 in Oregon Green 488 (OG) labeled AL/NP treated M2 macrophages.

5.6 In vitro laser microscopy

Primary macrophages were seeded in 4-well chamber slides (Thermo Fisher, Germany, Darmstadt) at a density of 10.000 cells per well and allowed to adhere overnight. Cells were polarized with 20 ng/mL interleukin 4 and 13 towards a M2-type for 24 h as described above. Equal to the previous performed *in vitro* cell uptake, M2-type macrophages were incubated with a final concentration of Oregon Green 488 labeled AL/NP, corresponding to 30 or 60 µM AL, or unloaded NP (corr. to ~60 µM AL) for 24 h, respectively.
Afterwards, cells were thoroughly washed with PBS and fixed with 4% formaldehyde for 15 min at 37 °C. Fixation solution was thoroughly rinsed off and chambers were detached from the slides as explained in detail by the manufacture's protocol. Cells were counterstained with DAPI from VECTASHIELD (Orton Southgate, UK) before cover slips were mounted together with mounting media (ProLong Antifade Mountants for Fixed Cells, Thermo Fisher, Germany, Darmstadt). Slides were subjected to laser microscopy (Leica, Germany, Wetzlar, Leica DMi8, DFC7000 T camera, Lumencor Light Engine).

5.7 Determination of TNFα by ELISA

As described above primary macrophages were seeded into 96-well plates at a density of 5000 cells per well and polarized towards a M2-type as described above. After polarization of 24 h, M2-type macrophages were incubated with AL/NP (corresponding to AL 10 or 30 µM), corresponding controls (AL, NP), or equal amounts of PBS for M2-type controls for 48 h. Afterwards, TNF**α** was quantified in the supernatant, using the TNFα Human ELISA Kit (Thermo Fisher, Germany, Dreieich) according to the manufacturer's protocol. In brief, standards, controls, and samples are added to the coated wells to allow the antigen from the samples bind to the immobilized antibody. After manual washing as described in the manufacturer's protocol and removal of excess antibody, a Streptavidin-horseradish peroxidase-labeled HRP (enzyme) is added, binding to the detection antibody. After further incubation and additional washing to remove unbound enzymes, a stabilized substrate is added, which reacts with the bound enzyme to produce color.
Absorbances was measured at 450 nm within 30 minutes of assay completion on an Infinite M200Pro spectrofluorometer (TECAN, Männerdorf, Switzerland).

6. *In Vivo* Studies

6.1 CCl_4 Fibrosis Model

All animal studies were approved by the local ethics committee on animal care (number 23177-07/612-1-007, Government of Rhineland Palatinate, Germany). 8-week-old female BALB/c mice (body weight ~ 20 g) were purchased from Charles River (Sulzfeld, Germany) and kept under 12 h light-dark cycles at 25 °C and 40–60% humidity with humane care. Mice had access to regular chow and water *ad libitum*. At predetermined time points mice were sacrificed by cervical dislocation. Carbon tetrachloride (CCl_4) (Honeywell, Seelze, US) diluted in mineral oil (v:v, 1:1) (Sigma-Aldrich, Darmstadt, Germany) was given by oral gavage 3 times a week in an escalating dose protocol (first dose 0.875 mL/kg; 1.75 mL/kg week 1; 2.5 mL/kg week 2, 3 and 4) as reported (6, 7). Mice gavaged with mineral oil alone served as non-fibrotic controls.

6.2 In Vivo Imaging of Near Infrared (NIR-)AL/NP

In vivo NIR fluorescence imaging of near infrared (NIR-) Dye 800RS-labeled AL/NP was performed with the IVIS Spectrum Imaging system (Caliper LifeSciences, Hopkinton, US). Fluorescence signal of NIR-AL/NP, NIR-AL and NIR-NP was routinely checked before injection and was found to be comparable between NIR-AL/NP and controls (compare **Fig. S22**). After injection at predetermined time points, fibrotic mice were transferred into the machine's image chamber and anesthetized temporarily with isoflurane. A picture integration time of 4 s was set for the fluorescence source. Filters were adjusted with excitation at 745 nm and emission at 800 nm to visualize NIR-AL/NP. Experiments were done on healthy and fibrotic mice providing similar results (**Fig. S26**).

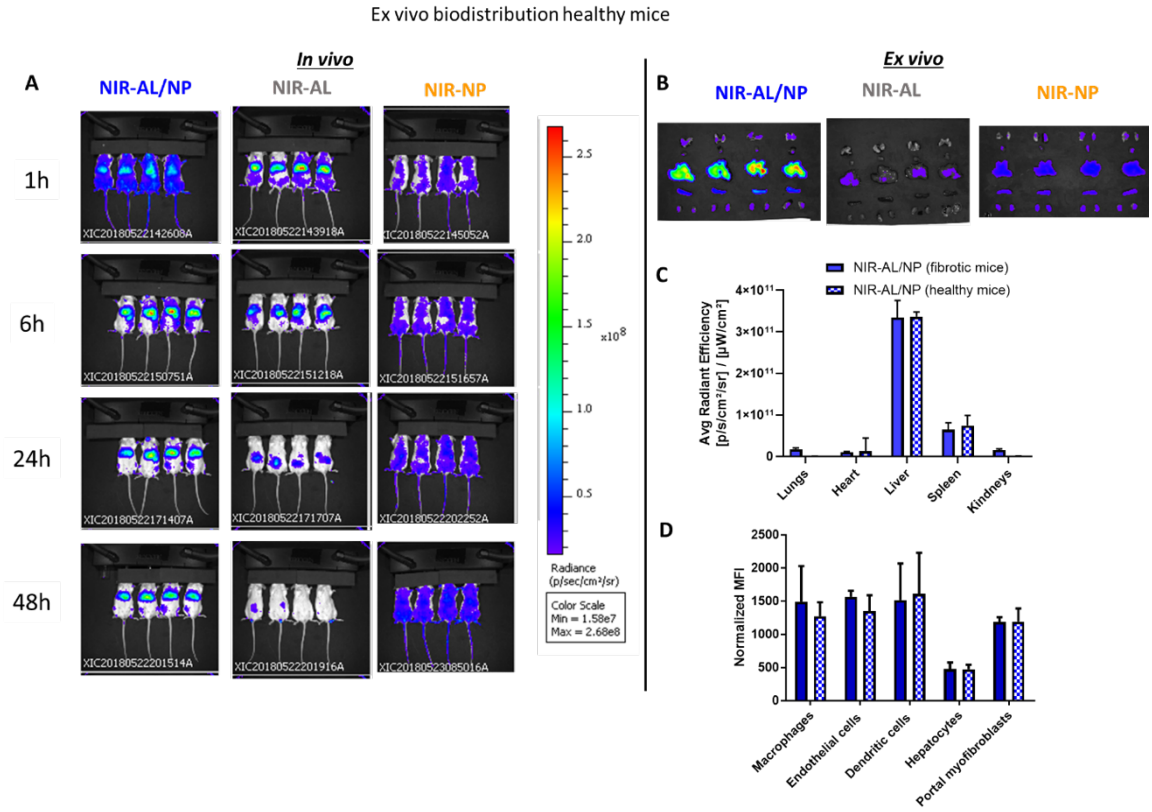

Fig. S28: Biodistribution of NIR-AL/NP in healthy mice compared to fibrotic mice. (A) *In vivo* biodistribution of NIR-AL/NP in healthy mice at 1, 6, 24 and 48 h after injection. (B) *Ex vivo* imaging of extracted organs from mice shown in A after 24 h. (C) Quantification of organ fluorescence of the extracted organs from healthy (B) and fibrotic (Fig. 3E) mice. (D) *In vivo* cellular uptake of NIR-AL/NP and controls in liver cells as quantified by FACS analysis of liver single cell suspension obtained from healthy (B) and fibrotic (Fig. 3E) mice.

6.3 Ex Vivo Imaging of Organs

24 h after the second injection of NIR-AL/NP mice were sacrificed and liver, spleen, lungs, heart and kidneys immediately transferred into the imaging chamber of the IVIS Spectrum Imaging system. Image acquisition was performed with the same settings as described above for *in vivo* imaging. To assess the accurate fluorescence intensity in the extracted organs, region-of-interests were drawn around the organs and fluorescence intensity was assessed by computerized fluorescence analysis, using the software of the IVIS machine provided by Caliper LifeSciences (Hopkinton, US).

6.4 Preparation of Liver Single Cell Suspensions

Directly after the *ex vivo* imaging (fibrotic) livers were digested according to the manufacturer's protocol (Preparation of single-cell suspensions from mouse liver, Milteny, Germany, Bergisch Gladbach). Briefly, livers were rinsed with PBS and after removal of the gall bladder digested with 5000 U/mL of collagenase IV (C5138, Sigma-Aldrich) in Krebs-Ringer-Buffer pH 7.4 according to the manufacturer's protocol. The livers were carefully homogenized with a gentleMACS™ dissociator (Milteny, Germany, Bergisch Gladbach) and incubated for 30 min at 37°C. The homogenization step was repeated, and the cell suspension filtered over a 100 µm cell strainer to remove non-digested liver compartments. The filtered cell suspension was transferred into new tubes and centrifuged at 300×g for 10 min at 4°C to collect all cells. The resulting supernatant was removed completely, and the remaining cell pellet was resuspended in 10 mL 1× Red Blood Cell Lysis Solution (Milteny, Germany, Bergisch Gladbach) for 5 min at RT and all cells were washed two times with PBS.

6.5 In Vivo Cellular Uptake of NIR-AL/NP

The liver cells obtained from mice injected with NIR-AL/NP were stained with fluorochrome conjugated cell specific antibodies to quantify cellular uptake of NIR-AL/NP by FACS analysis. The following antibodies were used: macrophages (CD45-FITC clone 30-F11, F4/80-PE clone BM8 and CD11b-PacificBlue clone M1/70); endothelial cells (CD31-PE clone MEC13.3), hepatocytes (Albumin-PE clone from #188835, R&D, Boston, USA), T-cells (CD3-PE clone 17A2), NK-T cells (NK-1.1-FITC clone PK136m, CD3-PE clone 17A2), dendritic cells (CD45-FITC clone 30-F11, F4/80-PE clone BM8, CD11c-Pacificblue clone N418) and portal myofibroblasts (PE-CD90.2 clone 53-2.1 from BDBioscience, Heidelberg, Germany). All antibodies were purchased from Biolegend if not mentioned otherwise. eFluor506 (eBioscience) was used to exclude dead cells. After cells were stained according to the manufacturer's protocol for surface staining, cells were fixed with 4% formaldehyde for 15 min at 37 °C and measured using a BD FACSCanto II (BDBioscience, Canada, Mississauga) Flow cytometer. Compensation was performed automatically by BD FACSDiva software version 7.0 with oneComp eBeads from eBioscience.10,000 cells were measured per staining. Further analysis of flow cytometry data was performed using open source Flowing Software 2.5.0 (Perttu Terho, Turku Centre for Biotechnology, Finland). Gating procedure was performed as shown in **Fig. S27**.

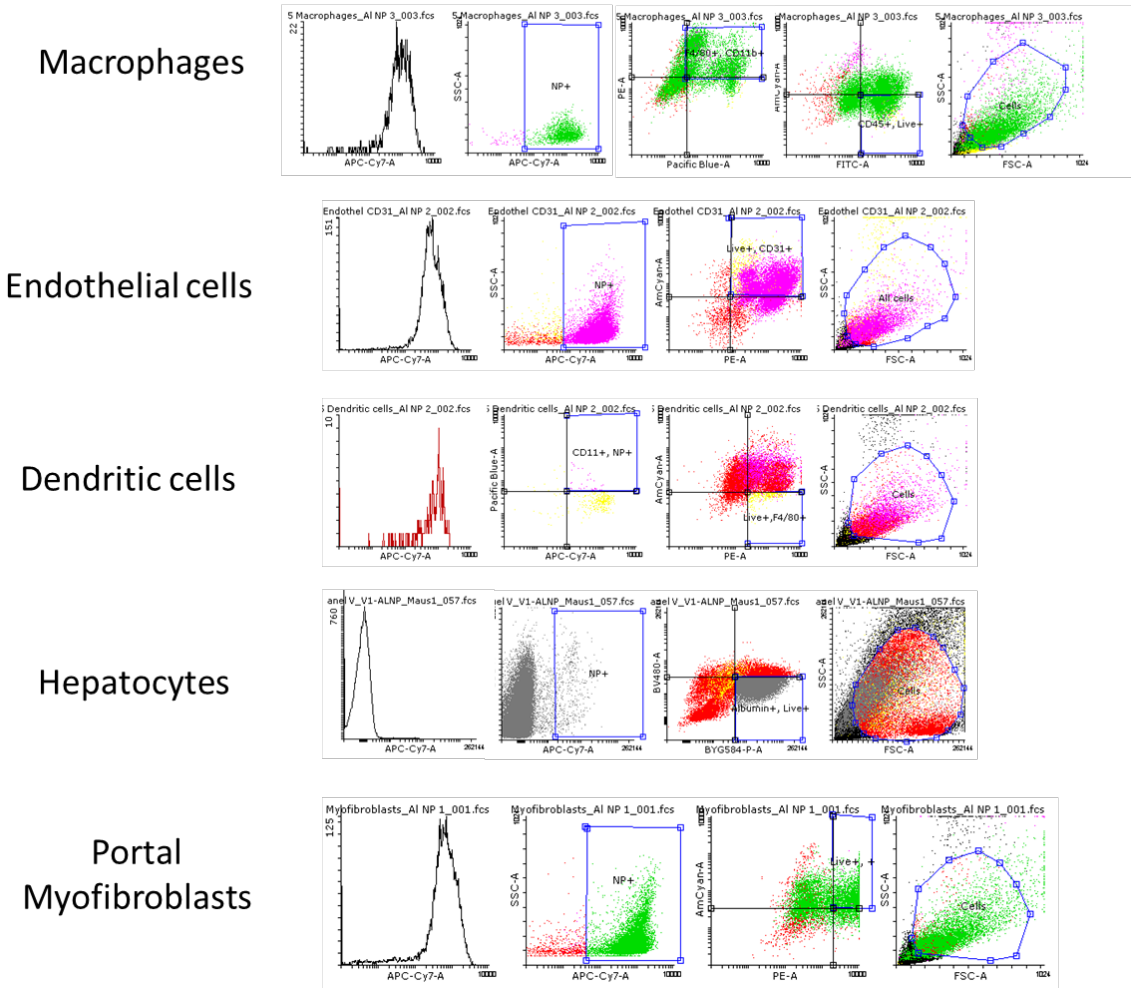

Fig. S29: Exemplary FACS gating procedure to determine the *in vivo* cellular uptake of NIR-AL-NP in (non-)parenchymal liver cells.

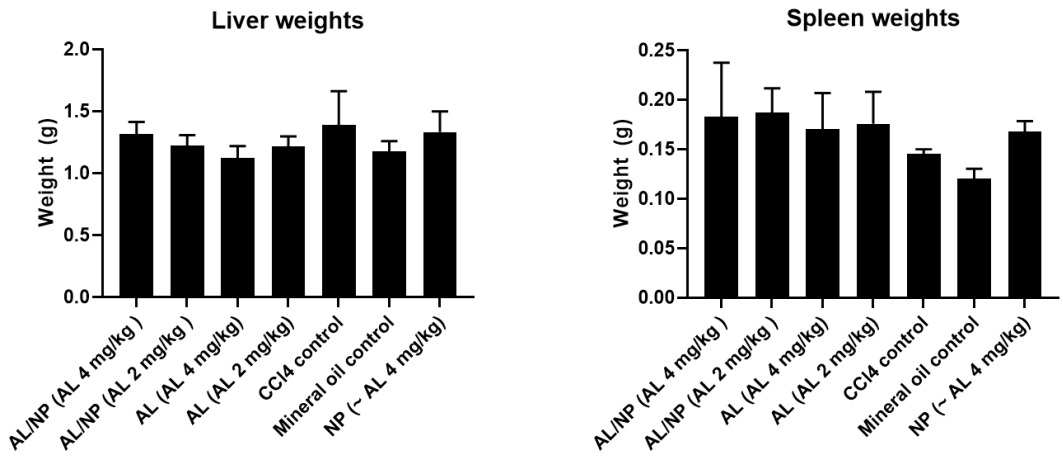

Fig. S30: Liver and spleen weights of CCl4 fibrotic mice treated with AL/NP and corresponding controls at sacrifice for *in vivo* antifibrotic treatment.

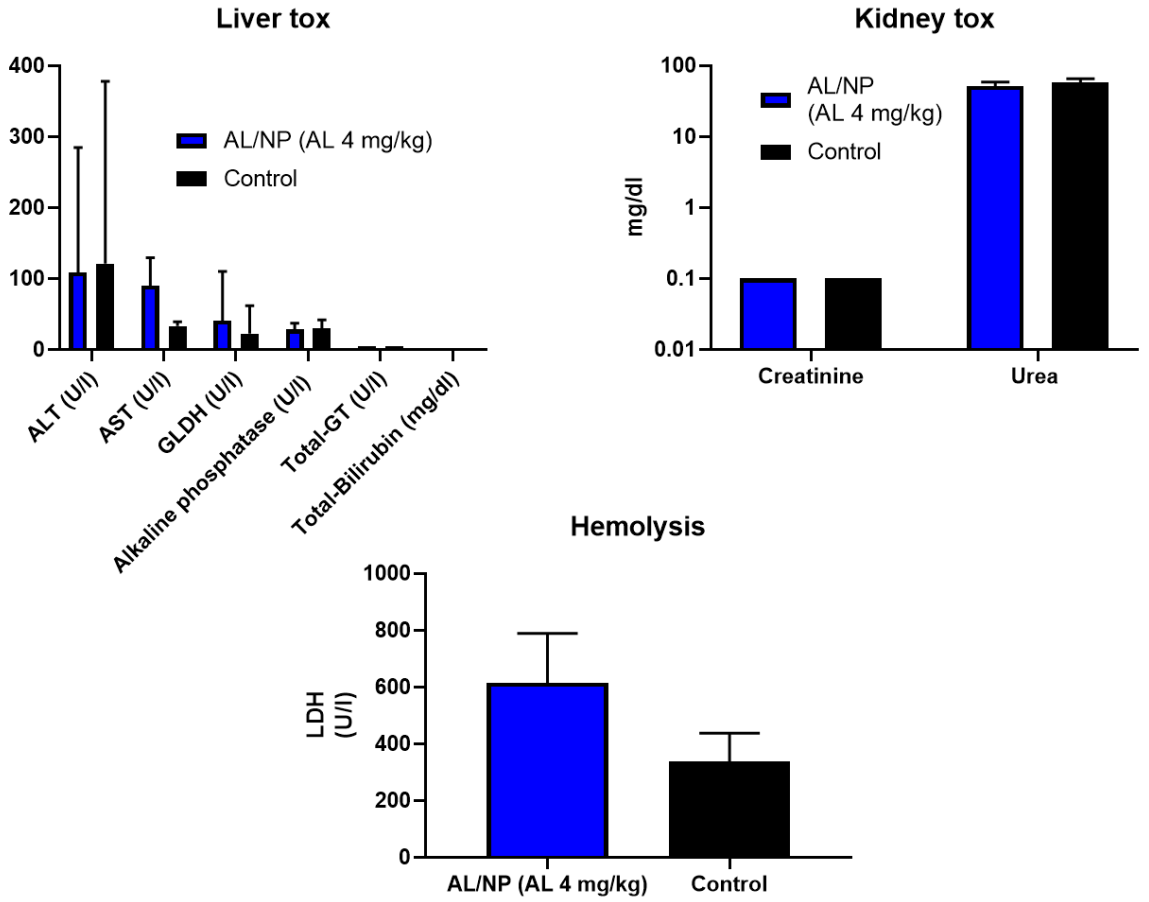

Fig. S31: *In vivo* biocompatibility of AL/NP. AL/NP showed no acute *in vivo* toxicity when mice were intravenously treated with a single high dose of AL/NP (4 mg/kg) after 24 h as assessed by routine laboratory safety parameters (n=5).

6.7 Hydroxyproline Determination

Liver collagen content was determined by absorption as total hydroxyproline as described recently (6, 7). Briefly, snap frozen liver specimens from the left, right and middle lobes, each weighing between 50 and 100 mg, were combined and homogenized in 3 mL of 6N HCl, followed by overnight hydrolysis at 110°C. Triplicates of 5 µL were placed in a transparent 96 well-plate (Greiner bio-one, Kremsmünster, Austria) and mixed with 50 µL of 0.1 M citrate buffer, pH 6.0, and 100 µL of 150 mg/mL chloramine T dissolved in citrate buffer (0.1 M, pH 6.0). After 30 min incubation at RT 100 µL of cooled Ehrlich's reagent (1.25 g of dimethyl-benzaldehyde dissolved in 100 mL distilled water) was added and incubated at 65 °C for 30 min. Absorbance was measured at 550 nm in an Infinite M200Pro spectrophotometer (TECAN, Grödig, Austria). Total hydroxyproline (µg/liver weight) was calculated on the basis of individual liver weights and the corresponding relative hydroxyproline content (µg/100 mg liver tissue). The assay data represent the average of two independent experiments.

6.8 Sirus Red Morphometry for Collagen

Formalin fixed liver sections were stained with H&E for 5 min, followed by 5% Picro-Sirius Red (Sigma-Aldrich, Darmstadt, Germany) at RT for 30 min and washed in distilled water and 0.5% acetic acid. 5 randomly selected fields (×100) were photographed using a Zeiss Scope A.1 microscope and an AxioCamMRC Zeiss camera (Jena, Germany) and the percentage of the Sirius Red-stained area was measured by Image J software with an adjusted threshold setting. For an accurate morphometrical quantification of collagen, portal areas were excluded and only parenchymal collagen deposition was quantified, representing the pathophysiologically relevant collagen deposition. Percentages of Sirius Red stained area in 5 randomly selected fields from each specimen, as assessed by computerized image analysis, are expressed as means ± SD (n = 5 per group; and n = 3 per sample) (6, 7).

6.9 Organ Histology and Immunohistochemistry

Specimens of excised livers were paraffin embedded and sectioned at 5 mm thickness. For histological assessment, deparaffinized liver sections were stained with hematoxylin (Merck, Darmstadt, Germany) and eosin Y (Carl Roth, Karlsruhe, Germany). For immunohistochemistry (IHC), deparaffinized organ sections were boiler-treated in 10 mM sodium citrate buffer pH 6.0 for 30 min, blocked with 10% goat serum, incubated with the primary antibody overnight at 4°C (α-SMA: ab124964 (1 µg/mL); CD206: ab64693 (0.05 µg/mL); CD68: ab125212 (0.25 µg/mL) – all Abcam, Cambridge, UK), treated with 3% hydrogen peroxide and incubated with a biotinylated anti-rabbit secondary antibody (Vector Laboratories, Burlingame, CA, USA) at a dilution of 1:500. Peroxidase activity was developed with an avidin-biotin-enzyme (DAKO), nuclei counterstained with hematoxylin, and sec- complex (ABC) (Vector Laboratories) and AECC chromogentions mounted with aqueous mounting media, Aquatex Ò (Merck, Darmstadt, Germany). Mounted sections were visualized using a Scope A.1 microscope and photomicrographed with an AxioCam MRC camera (Carl Zeiss Microscopy, Jena Germany). For quantification of positively stained cells in sections treated with the corresponding antibodies were manually counted in 5 randomly selected fields from each specimen. This procedure was repeated twice per sample and resulting numbers are expressed as means ± SD.

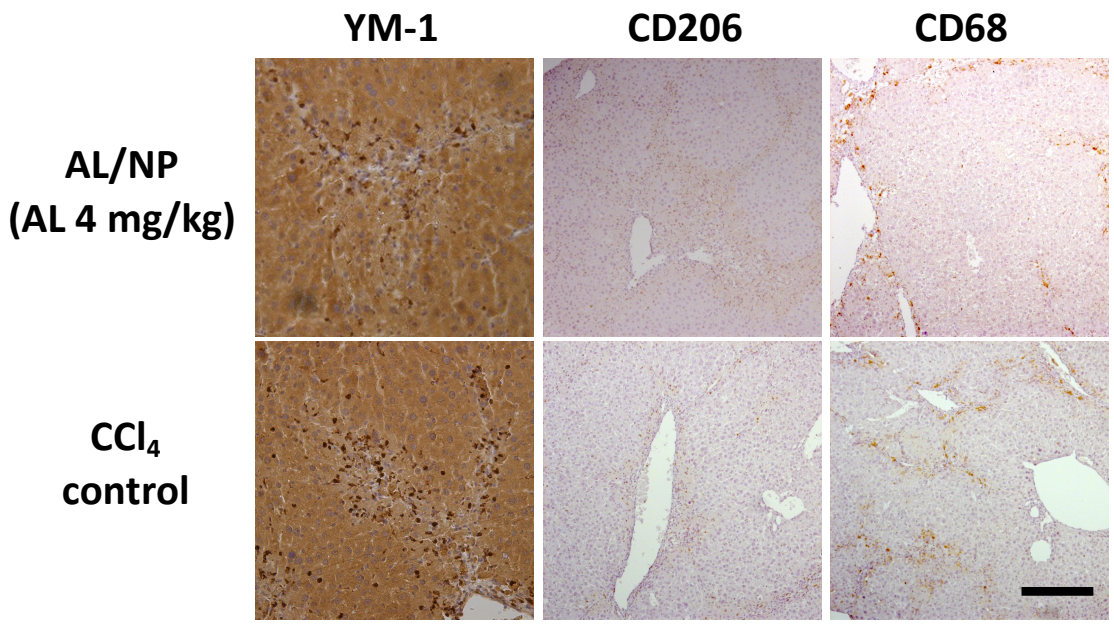

Fig. S32: In liver sections stained for the pan-macrophage marker CD68 or the M2 markers YM-1 and CD206, respectively, AL/NP treatment significantly reduced the M2 markers, while CD68 was not affected (scale bare 200 μm).

6.10 Genomics

The RNA-seq data presented in this manuscript has been deposited in NCBI's Gene Expression Omnibus and are accessible through GEO series accession number GSE185997 https://www.ncbi.nlm.nih.gov/geo/query/acc.cgi?acc=GSE185997.

6.10.1 Total RNA extraction, library preparation and directional mRNA sequencing

Total RNA was extracted from fresh frozen pieces of mouse liver using Qiagens RNeasy Mini Kit. Quantity and quality were assessed using the Qubit 3 fluorometer with the RNA BR AssayKit (Invitrogen) and the Agilent Bioanalyzer 2100 system using the RNA Pico kit. mRNA-focused RNA libraries were prepared using Illumina's TruSeq stranded RNA library prep kit with an input amount of 1000 ng total RNA. Poly(A)-positive mRNA transcripts were isolated from total RNA by binding to magnetic oligo(d)T beads and subsequently fragmented and reverse transcribed during first and second strand synthesis to yield double-stranded cDNA. The ends of the cDNA molecules were end repaired and an adenosine overhang was added to all 3' ends (A-tailing step) to facilitate the ligation of the adapter molecules. These adapters have individual dedicated index sequences and add the Illumina specific sequences that are needed for amplification, flow cell hybridization and sequencing. 8 bp single-index NEXTflex DNA barcodes (Perkin Elmer) were used. The final ligation product was amplified via PCR. Intermediate and final library purification steps were done using AMPure XP beads (Beckman Coulter). Final library quantity and quality was done using the Qubit 3 fluorometer with the dsDNA HS AssayKit (Invitrogen) and the Agilent Bioanalyzer 2100 system using the High Sensitivity DNA kit. All mRNA libraries were sequenced in paired-end mode (2 x 50 nt) on an Illumina NovaSeq 6000 instrument resulting in around 30 million distinct sequencing read pairs per library.

6.10.2 Differential expression analysis and principal component analysis

RNA-seq raw reads were subject to quality control with FastQC (www.bioinformatics.babraham.ac.uk/projects/fastqc/), and subsequently aligned with STAR (v 2.6.1a) (9) to the mouse genome (Mus musculus GRCm38). Gene expression values were quantified using featureCounts (10) against the ENSEMBL annotation (Release 76). The read counts table was processed for Exploratory Data Analysis with pcaExplorer (v 2.12.0) (11), and input for the DESeq2 differential expression analysis framework (v1.26.0) (12). Log2 fold change values after "apeglm" shrinkage (13) are shown.
Principal component analysis (PCA) was performed on the variance stabilized count data with pcaExplorer's pcaplot function. The ideal package by Marini et al. (v1.10.0) (14) was used to carry out the differential expression analysis, while the GeneTonic package by Marini et al. (v1.0.0) (15) was used to assist the data interpretation after the functional enrichment analyses.

RNA-seq reads were processed with kallisto (v0.42.4) (9) and Mus musculus reference GRCm38 (Ensembl release 84). Estimated read counts were summarized per gene and used for differential expression analysis with DESeq2 (v1.24.0) (10). Log2 fold change values after "apeglm" shrinkage (11) are shown.
Principal component analysis (PCA) was performed on the variance stabilized count data with DESeq2's plotPCA function.

6.10.3 Ingenuity Pathway Analysis®

The networks analyses were performed with the Ingenuity Pathway Analysis® (IPA®, Qiagen, Netherlands). For that, differential gene expression data was uploaded and significantly differentially expressed genes with cut-offs of | log2 Fold Change (FC) | >= 1 and False Discovery Rate (FDR) < 0.05 were selected for analysis.

6.10.4 Gene Set Enrichment Analysis

Gene set enrichment analysis was performed to identify enriched molecular signatures between AL/NP (AL 4 mg/kg) treated vs. CCl_4-fibrotic mice as reported by us before (12). For this purpose, the Gene Set Enrichment Analysis (GSEA) tool was applied using the Molecular Signatures Database (MSigDB v6.0) with Hallmark gene sets for inflammatory response (HALLMARK_INFLAMMATORY_RESPONSE) and immunologic signatures of macrophages M1 vs. M2 phenotypes (COATES_MACROPHAGE_M1_VS_M2_UP) (12-14).

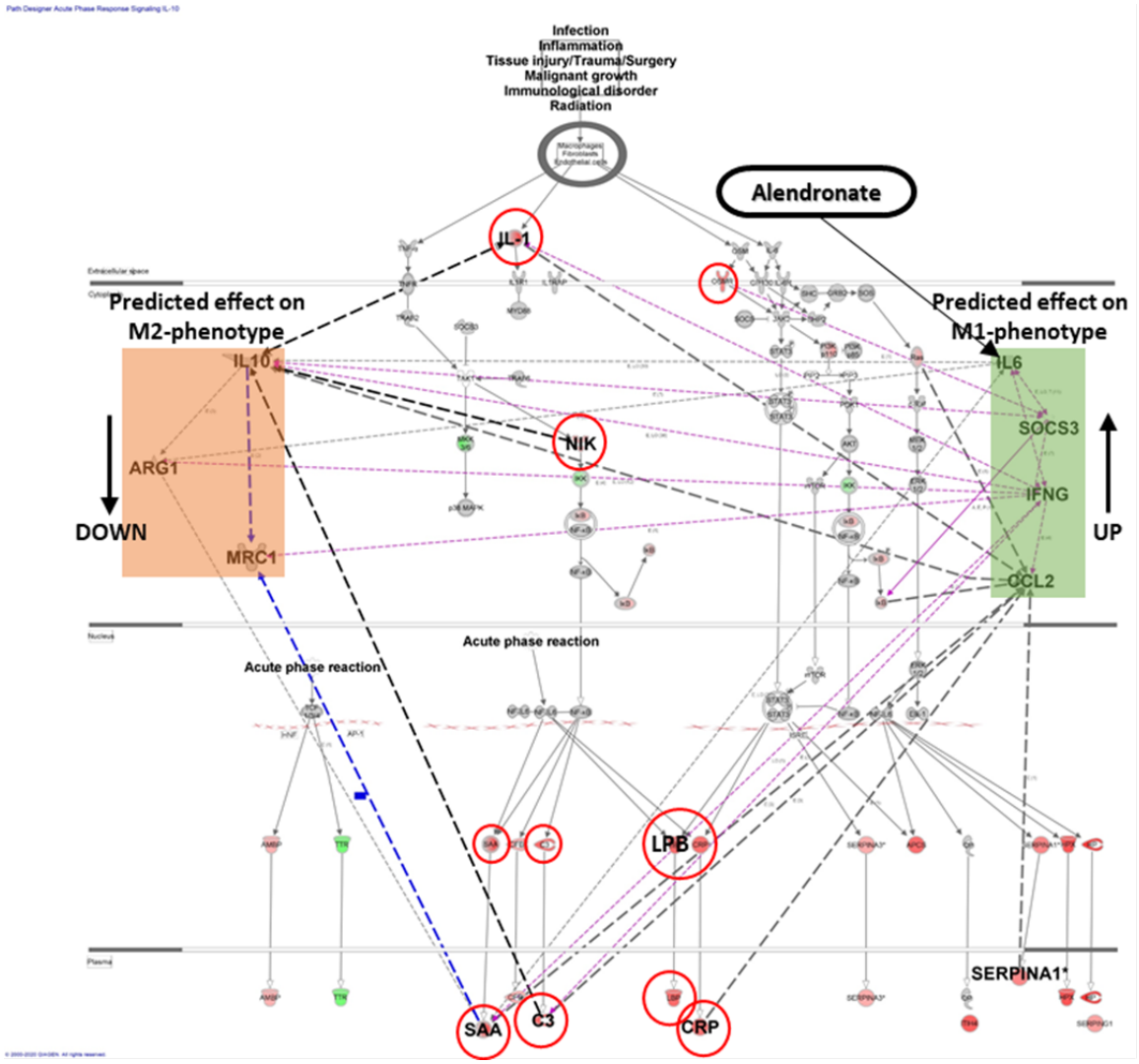

Fig. S33: The acute response phase signaling pathway, which was determined to be activated as predicted by IPA®. The prediction is based on key genes, which are present downstream in the pathway and were found to be significantly upregulated in the dataset (corresponding key genes circled in red). Further, M2 macrophage phenotype markers are predicted to be downregulated by the upregulated key genes, while M1 markers are increased.

6.11 Proteomics

6.11.1 Protein digestion

Proteins were digested according to the FASP (filter-aided sample preparation) protocol, described in detail (15-17). Frozen liver samples at a size of 1 x 1 mm were lysed in 200 µl FASP-Lysis-buffer (7 M urea, 2 m Thio Urea, 5 mM Dithithreitol (DTT), 2% (w/v) CHAPS) and 15 cycles (30 s sonication, 30 s break each cycle) in a Bioruptor (Diagenode, Liège, Belgium). After determining the protein concentration using the Pierce 660 nm protein assay (Thermo Fisher Scientific) 20 µg sample were loaded onto spin filter columns (Nanosep centrifugal devices with Omega membrane, 30 kDa MWCO; Pall, Port Washington, NY) and washed three times with wash buffer (8 M Urea, 0.1 M TRIS-Base) to remove detergents. Proteins were then reduced by adding 8 mM DTT, alkylated with 50 mM Iodoacetamide (IAA) and excessive IAA was quenched, again using 8 mM DTT. After three washes in 50 mM NH4HCO3 proteins were digested overnight at 37°C using trypsin (Trypsin Gold, Promega, Madison, WI) at an enzyme-to-protein ratio of 1:50 (w/w). Peptides were recovered by centrifugation, mixed with 10% TFA and washed once with 50 mM NH_4HCO_3. The obtained flow-through was lyophilized and finally brought to a final concentration of 0.2 µg/µl in 0.1% FA.

7.2 LC-MS analysis

Liquid chromatography (LC) of tryptic peptides was performed on a NanoAQUITY UPLC system (Waters Corporation, Milford, MA) equipped with 75 µM x 250 mm HSS-T3 C18 column (Waters corporation). Mobile phase A was 0.1% (v/v) formic acid (FA) and 3% (v/v) dimethyl sulfoxide (DMSO) in water. Mobile phase B was 0.1% (v/v) FA and 3% (v/v) DMSO in acetonitrile (ACN). Peptides were separated running a gradient from 5 to 60% (v/v) mobile phase B at a flow rate of 300 nL/min over 120 min. The column was heated to 55 °C. MS analysis of eluting peptides was performed by data-independent acquisition (DIA) in UDMSE as described previously (15). In brief, precursor ion information was collected in low-energy MS mode at a constant collision energy of 4 eV. Fragment ion information was obtained in the elevated energy scan applying drift-time specific collision energies. The spectral acquisition time in each mode was 0.6 s with a 0.05 s-interscan delay resulting in an overall cycle time of 1.3 s for the acquisition of one cycle of low and elevated energy data. [Glu1]-fibrinopeptide was used as lock mass at 100 fmol/µL and sampled every 30 s into the mass spectrometer via the reference sprayer of the NanoLockSpray source.

7.3 Data Processing and Label-Free Quantification

Raw UDMSE data processing and database search was performed using ProteinLynx Global Server (PLGS, ver. 3.0.2, Waters Corporation). The resulting proteins were searched against UniProt Mouse proteome database (UniProtKB release 2018_09, 16991 entries) supplemented with a list of common contaminants. The database search was specified by trypsin as enzyme for digestion and peptides with up to two missed cleavages were included. Furthermore, Carbamidomethyl cysteine was set as fixed modification and oxidized methionine as variable modification. False discovery rate (FDR) assessment for peptide and protein identification was done using the target-decoy strategy by searching a reverse database and was set to 0.01 for database search in PLGS.

Retention time alignment, exact mass retention time (EMRT), as well as normalization and filtering were performed in ISOQuant ver.1.8 (18). By using TOP3 quantification (19), absolute in-sample amounts of proteins were calculated. Statistical analysis was done in Perseus (20) by performing two-tailed, paired -tests and subsequent Benjamini-Hochberg correction (21). Q-values < 0.05 were considered as significant.

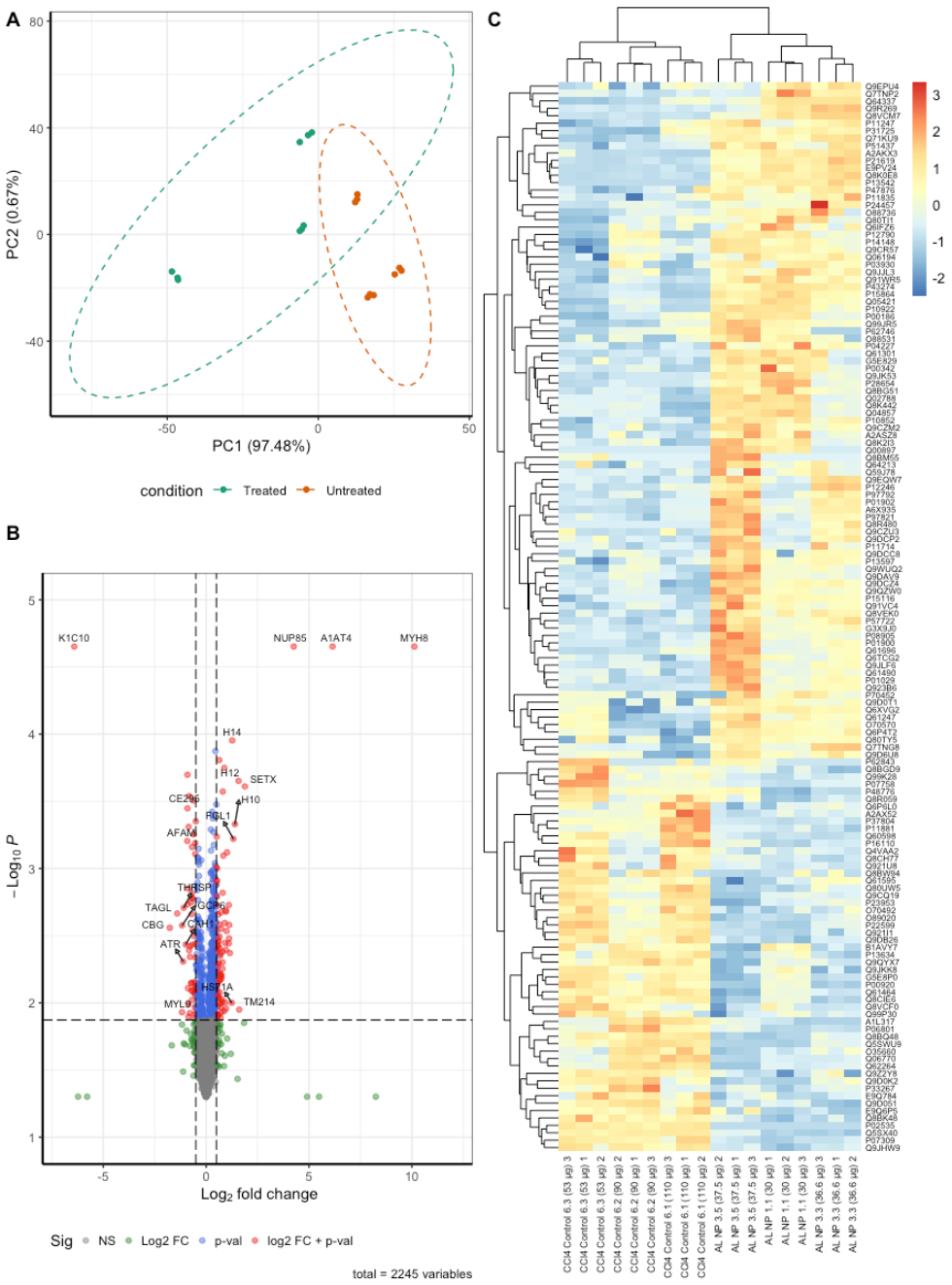

Fig. S34: Mass spectrometry results of AL/NP treated and untreated fibrotic mice. A: Principal component analysis. B: Volcano plot. C) Heatmap reflecting the relative changes in protein expression for significantly regulated proteins with Δ0.5 log2 ratio (red dots in B).

Supplementary References

1. G. R. Kieczykowski, *et al.*, Preparation of (4-Amino-1-Hydroxybutylidene)bisphosphonic Acid Sodium Salt, MK-217 (Alendronate Sodium). An Improved Procedure for the Preparation of 1-Hydroxy-1,1-bisphosphonic Acids. *J. Org. Chem.* **60**, 8310–8312 (1995).
2. A. Huppertsberg, *et al.*, Squaric Ester-Based, pH-Degradable Nanogels: Modular Nanocarriers for Safe, Systemic Administration of Toll-like Receptor 7/8 Agonistic Immune Modulators. *J. Am. Chem. Soc.* **143**, 9872–9883 (2021).
3. K. Rausch, A. Reuter, K. Fischer, M. Schmidt, Evaluation of Nanoparticle Aggregation in Human Blood Serum. *Biomacromolecules* **11**, 2836–2839 (2010).
4. N. Leber, *et al.*, α-Mannosyl-Functionalized Cationic Nanohydrogel Particles for Targeted Gene Knockdown in Immunosuppressive Macrophages. *Macromol. Biosci.* **19** (2019).
5. L. Kaps, *et al.*, In Vivo siRNA Delivery to Immunosuppressive Liver Macrophages by α-Mannosyl-Functionalized Cationic Nanohydrogel Particles. *Cells* **9**, 1905 (2020).
6. N. Leber, *et al.*, SiRNA-mediated in vivo gene knockdown by acid-degradable cationic nanohydrogel particles. *J. Control. Release* **248**, 10–23 (2017).
7. L. Kaps, *et al.*, In Vivo Gene-Silencing in Fibrotic Liver by siRNA-Loaded Cationic Nanohydrogel Particles. *Adv. Healthc. Mater.* **4**, 2809–2815 (2015).
8. C. Hörtz, *et al.*, Cylindrical Brush Polymers with Polysarcosine Side Chains: A Novel Biocompatible Carrier for Biomedical Applications. *Macromolecules* **48**, 2074–2086 (2015).
9. N. L. Bray, H. Pimentel, P. Melsted, L. Pachter, Near-optimal probabilistic RNA-seq quantification. *Nat. Biotechnol.* **34**, 525-527 (2016).
10. M. I. Love, W. Huber, S. Anders. Moderated estimation of fold change and dispersion for RNA-seq data with DESeq2. *Genome Biol.* **15**, 550 (2014).
11. A. Zhu, J. G. Ibrahim, M. I. Love. Heavy-tailed prior distributions for sequence count data: removing the noise and preserving large differences. *Bioinformatics* **35**, 2084-2092 (2019).
12. F. Foerster, *et al.*, Enhanced protection of C57 BL/6 vs Balb/c mice to melanoma liver metastasis is mediated by NK cells. *Oncoimmunology* **7**, e1409929 (2018).
13. A. Subramanian, *et al.*, Gene set enrichment analysis: A knowledge-based approach for interpreting genome-wide expression profiles. *Proc. Natl. Acad. Sci.* **102**, 15545–15550 (2005).
14. P. J. Coates, J. K. Rundle, S. A. Lorimore, E. G. Wright, Indirect Macrophage Responses to Ionizing Radiation: Implications for Genotype-Dependent Bystander Signaling. *Cancer Res.* **68**, 450–456 (2008).
15. U. Distler, J. Kuharev, P. Navarro, S. Tenzer, Label-free quantification in ion mobility-enhanced data-independent acquisition proteomics. *Nat. Protoc.* **11**, 795–812 (2016).
16. M. Sielaff, *et al.*, Evaluation of FASP, SP3, and iST Protocols for Proteomic Sample Preparation in the Low Microgram Range. *J. Proteome Res.* **16**, 4060–4072 (2017).
17. J. R. Wiśniewski, A. Zougman, N. Nagaraj, M. Mann, Universal sample preparation method for proteome analysis. *Nat. Methods 2009 65* **6**, 359–362 (2009).
18. U. Distler, *et al.*, Drift time-specific collision energies enable deep-coverage data-independent acquisition proteomics. *Nat. Methods* **11**, 167–170 (2014).
19. J. C. Silva, M. V. Gorenstein, G. Z. Li, J. P. C. Vissers, S. J. Geromanos, Absolute quantification of proteins by LCMSE: a virtue of parallel MS acquisition. *Mol. Cell. Proteomics* **5**, 144–156 (2006).
20. S. Tyanova, J. Cox, Perseus: A Bioinformatics Platform for Integrative Analysis of Proteomics Data in Cancer Research. *Methods Mol. Biol.* **1711**, 133–148 (2018).
21. Y. Benjamini, Y. Hochberg, Controlling the False Discovery Rate: A Practical and Powerful Approach to Multiple Testing. *J. R. Stat. Soc. B* **57**, 289–300 (1995).